Original Article

Comparative Study of the Therapeutic Effect of Platelet Rich Plasma Versus Bone Marrow Derived Mesenchymal Stem Cells on Acute Skeletal Muscle Injury of Adult Male Albino Rats

Rana Saad[1], Wahid M. Stephanos[1], Anisa Meleis[1], Samar S Ibrahim[2] and Iman Nabil[1]

[1]Department of Histology and Cell Biology, [2]Center of Excellence for Research in Regenerative Medicine and Applications (CERRMA), Faculty of Medicine, Alexandria University, Egypt

ABSTRACT

Introduction: Skeletal muscle injuries are common in athletes, however, no effective treatment is available. Platelet rich plasma (PRP) and mesenchymal stem cells (MSCs) have been used in treatment of different musculoskeletal disorders. However, a hot debate has been raised regarding the deleterious effect of PRP injection following muscle injury.

Aim of the Work: To compare the therapeutic effect of PRP versus bone marrow derived-MSCs in the treatment of acute injury in rats' skeletal muscle.

Materials and Methods: 52 adult rats were utilized for the whole study, 32 rats as experimental groups, 10 rats for PRP production, and 10 rats for MSCs isolation. MSCs were characterized morphologically and by flow cytometer. The 32 rats were divided into: group I (control), the other 3 groups underwent induced quadriceps femoris muscle injuries without further treatment in group II (untreated injured) or followed 2 hours later on by a single intramuscular injection of either PRP in group III or BM-MSCs in group IV respectively. After 21 days, the rats were sacrificed. The muscles were obtained for biochemical and histological investigations. Tissue homogenates were used to measure the levels of myoblast determination protein 1 (MyoD), skeletal troponin I (sTnI), malondialdehyde (MDA), superoxide dismutase (SOD), glutathione reductase (GSH) and total antioxidant capacity (TAC). Muscle specimens were processed and examined by light and electron microscopies. Masson's trichrome-stained sections were subjected to morphometric analysis. Statistical analyses were done.

Results: Induced muscle injuries resulted in damage to the myofibers, vacuolation, cellular infiltration, damaged sarcolemma, abnormal nuclei, pleomorphic mitochondria, distorted triads, a significant increase in collagen deposition, sTnI, and MDA together with reduction in MyoD and antioxidant enzymes. The PRP-treated group showed a mixture of muscle damage and regeneration. Meanwhile, MSCs revealed better regeneration apart from a few degenerative foci.

Conclusion: BM-MSCs injection showed superb muscle regeneration with less fibrosis compared to PRP.

Received: 11 September 2023, **Accepted:** 23 October 2023

Key Words: Histology, mesenchymal stem cells, MyoD, platelet rich plasma, skeletal muscles.

Corresponding Author: Rana Saad, PhD, Department of Histology and Cell Biology, Faculty of Medicine, Alexandria University, Egypt, **Tel.**: +20 10 2077 2688, **E-mail:** rana.anwr@yahoo.com

ISSN: 1110-0559, Vol. 47, No. 4

INTRODUCTION

Skeletal muscle injuries are very prevalent in athletes, particularly during vigorous exercise. Such injuries result from contusion, strain or even laceration[1]. The pattern of these injuries can happen in an acute manner or as a result of repetitive traumas over a period of time[2]. Following an injury, muscle tissue undergoes a process of healing which is the same in the majority of muscle injuries. Nonetheless, this process is incomplete due to the development of non-contractile fibrotic tissue, two weeks following the injury. The formed scar tissue is structurally and functionally inferior to normal muscle fibre and thus, susceptible to re-injury[3]. Eventually, substantial morbidity like mechanical deficit, atrophy or contracture often happens after such injuries[4].

The regular management applied for muscle injuries includes bed rest, protection, ice compression and elevation, in addition to medications such as analgesics or even corticosteroids. The aim of these modalities is symptomatic control, limitation of muscle damage and stimulation of the own muscle regenerative response. Nevertheless, their efficacies are not proven in the treatment of acute muscle injuries[5].

Accordingly, there has been a growing concern in the application of regenerative medicine techniques such as platelet rich plasma (PRP) and stem cells in the treatment of different musculoskeletal disorders[6,7]. PRP is obtained from autologous blood and has been recommended for treatments of sports injuries as it promotes tissue repair. Owing to its high contents of different beneficial growth factors, PRP is documented to have a tremendous healing potential when injected locally into the injured tissue. These growth factors enhance the process of tissue repair via recruiting different types of cells participating in the healing mechanism, promoting their proliferation and differentiation with the subsequent acceleration of the reparative process with better results[8].

DOI: 10.21608/ejh.2023.234951.1944

Even with the widespread use of PRP in acute muscle injury, a hot debate has been raised regarding the deleterious effect of PRP injection following muscle injury[9,10]. PRP treatment was reported to increase considerably the levels of other pro-inflammatory cytokines particularly transforming growth factor-β1 (TGF-β1) which has been associated with inhibition of myogenic differentiation and enhancement of fibrous tissue formation[11]. However, in *vivo* studies validate that the effect of TGF-β1 on satellite cells is variable determined by the simultaneous existence of other growth factors[9]. Consequently, more caution has to be considered when recommending PRP treatment for muscular injuries.

Currently, stem cell therapies appear to attract a wider range of attention as regenerative medicine tools and promise to hold the potential for the treatment of muscle injuries[12]. Particularly, mesenchymal stem cells (MSCs) can revive damaged tissue through different mechanisms including paracrine effect, myogenic differentiation potential, and immunomodulation with the net result of suppressing tissue damage and fibrosis, promoting growth and activating, recruiting as well as increasing resident population of tissue stem cells[13].

Therefore, the present study was conducted to compare the therapeutic effect of PRP versus bone marrow-derived MSCs (BM-MSCs) in the treatment of acute injury in adult male albino rats' skeletal muscles.

MATERIAL AND METHODS

This study was conducted on fifty-two male Sprague Dawley rats, aged 6-8 weeks, weighing about 150- 200 g. Thirty-two rats served as the experimental groups while the other twenty rats were divided equally for obtainment of PRP and BM-MSCs respectively. The experimental rats were raised at the Animal House of the Physiology department, Alexandria Faculty of Medicine. A controlled environment was prepared including temperature of 22 ± 3ºC, 12-h light/dark cycles, and air humidity of 55 ± 10%. They were freely fed on regular laboratory food and water. All procedures were approved by the Local Medical Ethics Committee (IBN NO: 00012098, FWA NO; 00018699, Serial Number: 0201543), Faculty of Medicine, Alexandria University, and in line with the criteria of care and use of laboratory animals.

The thirty-two experimental rats were randomized into four equal groups (n=8):

Group I (Control): Uninjured rats served as a control group for obtaining quadriceps femoris muscle specimens from the same anatomical area as the injured one.

The rest of the animals (24 rats) received a single intramuscular (IM) injection of 80 mg/Kg phenobarbital[14] and then underwent non penetrating traumatic events at multiple successive levels in a transverse direction along the length of the quadriceps femoris muscle of both hind limbs using a curved artery forceps (Aesculap, Tuttlingen, Germany) with jaws protected by polyethylene tubes and closed for 20 seconds[15].

The injured animals were distributed into:

Group II (Untreated injured): The injured rats of this group didn't receive any treatment.

Group III (PRP-treated): Each rat received a single IM injection of PRP solution (100 µL) two hours after injury[16].

Group IV (BM-MSCs-treated): Each rat received a single IM injection of 1x106 BM-MSCs in 1 ml of complete culture medium (CCM) two hours after injury[17].

Production of PRP

This procedure was done at The Clinical Pathology department, Faculty of Medicine, Alexandria University. The whole blood was drawn from ten rats via an ocular vein under general anaesthesia (IM injection of 100 mg/Kg phenobarbital)[18] and collected in blood tubes containing citrate phosphate dextrose. Centrifugation of the blood at 1000 rpm at 4°C for 15 minutes, then a rest period of 5 minutes, and finally re-centrifugation at 1000 rpm at 4°C for 15 minutes were performed. After the first centrifugation, separation of the plasma from the red blood cell cells was achieved. During the second centrifugation, discarding of the supernatant portion was done to obtain a small fraction which is about 1 ml of the remained heavier centrifuged material which was the platelet concentrate or PRP. Using a pipette, aspiration of the platelet-rich fraction of the supernatant was done and maintained at room temperature. Determination of the final platelets' concentration in the PRP was performed by an automated cell counter. The concentration must be at a minimum of 4 times the whole blood level[19].

Isolation and culture of BM-MSCs

This procedure was done at the Center for Excellence for Research in Regenerative Medicine and its Applications (CERRMA). Ten animals were euthanized by a single IM injection of 100 mg/Kg phenobarbital[18]. Both tibia and femur were exteriorized for flushing the bone marrow using 5 ml of CCM; composed of low glucose Dulbecco's modified Eagle's medium (LG-DMEM, Sigma-Aldrich) supplemented with 20% foetal bovine serum (FBS, Sigma-Aldrich), 2 mM L-glutamine (Lonza) and 1% penicillin/streptomycin (P/S, Lonza). Flushed bone marrow was centrifuged for 5 minutes at 1200 rpm. The resultant pellets were cultured in CCM onto a 25 cm 2 tissue culture flask and finally incubated in the CO_2 incubator at 37o C with 5% CO_2 and 95% O^2. Every three days, the growth medium was changed and replaced with a fresh one after washing the cells three times with phosphate buffer saline (PBS, Lonza). Daily examination of the cultured cells was done using phase contrast inverted microscopy till reaching sufficient confluency (80% at day 10 of primary culture; passage 0; p0). Subsequent passages were done till passage 3 (p3)[20].

Colony forming unit-fibroblast (CFU-F) assays

About one hundred cells at p3 were plated in six-well plates in CCM. The cells were kept in CCM for two weeks at the CO_2 incubator, with the media changed twice weekly. On day 14, washing of the cells with PBS was done followed by fixation in 100% methanol for 5 minutes. In order to distinguish colonies, the cells were incubated in 3% crystal violet solution (Sigma-Aldrich) in 100% methanol for 30 minutes at room temperature, followed by washing the plates twice with distilled water and then left to dry. Counting the number of colonies was done to calculate plating efficiency (CFU potential) as follows: Plating efficiency = (Number of colonies / Number of cells plated) X 100. Using the phase contrast inverted microscopy, the number of colonies exhibiting five or more cells was scored. A CFU potential of over 40% indicates a good culture of BM-MSCs[21].

Immunophenotyping characterization of BM-MSCs using the flow cytometer

The cells were characterized using cell surface markers by staining the cells with different fluorescent-labeled monoclonal antibodies. BM-MSCs characterized for CD44 and CD90 as positive markers, in addition to CD45 (hematopoietic surface marker), as a negative marker. Detachment of the cultured cells was done with 0.25% trypsin-EDTA solution (Thermo Fisher Scientific). The cultured cells were washed with PBS and then incubated for 30 minutes in the dark at room temperature, with monoclonal Allophycocyanin-conjugated antibody for CD44 and CD90 (Anti-Thy1.1) (Abcam, UK) and monoclonal phycoerythrin (PE)-conjugated antibody for CD45 (Abcam, UK). Analysis of the immunofluorescence on the viable cells was performed using Becton Dickinson, fluorescent activated cell sorting (FACS) calibre flow cytometer equipped with cell Quest software[22].

Injection of PRP

Two hours after injury, each rat of the PRP-treated group (group III) was injected once with 100 µl of PRP into the site of injury using an insulin syringe. Each dose was injected respectively into each limb. Activation of PRP by calcium gluconate was done before the injection[16].

Injection of BM-MSCs

Two hours after injury, each rat of the BM-MSCs-treated group (group IV) was locally injected once with a single dose of 1x106 BM-MSCs suspended in 1 ml CCM using an insulin syringe. Each dose was respectively injected into the right and the left limbs[17].

The whole experiment was terminated 3 weeks from the day of injury (day 0), and all the rats were sacrificed by IM injection of 100 mg/Kg phenobarbital[18]. The right quadriceps femoris muscles were processed for the light microscopic examination, while small specimens were excised from the left sides and processed to obtain tissue homogenate for biochemical study and the remaining parts were processed for electron microscopic examination.

Biochemical study

Tissue homogenates were prepared for biochemical analysis[23]. All the procedures were done at the Biochemistry department, Faculty of Medicine, Alexandria University.

Measurement of biochemical markers for muscle damage and regeneration

The tissue levels of Myoblast determination protein 1 (MyoD); a marker for muscle regeneration and skeletal troponin I (sTnI); a biomarker for muscle damage were measured using Enzyme-linked immunosorbent assay (ELIZA) according to the manufacture's protocol.

Measurement of lipid peroxidation and antioxidants markers

Colorimetric assay was used to measure the tissue levels of lipid peroxidation using a malondialdehyde (MDA) assay kit as well as the antioxidant markers including superoxide dismutase (SOD), reduced glutathione (GSH) and the total antioxidant capacity (TAC) using assay kits according to the manufacture's protocol.

Histological examination

a-Light microscopy (LM): The right quadriceps femoris muscles were immersed in 10% formol saline and then processed to obtain 5-6 µm thick paraffin sections stained with Haematoxylin and Eosin (H&E) and Masson's trichrome[24]. The obtained stained sections were examined by LM and photographed. To measure the area percentage of collagen, six random images were manually selected from Masson's trichrome-stained sections and imaged using a 10x objective lens. Using Image J software (version 1.51k, Wayne Rasband, National Institutes of Health, USA), images were viewed and the colour was analysed by the colour threshold tool and the pixels were measured[25].

b-Transmission electron microscopy (TEM): Specimens from the left quadriceps femoris muscles were cut into small pieces (about 1/2- 1 mm3), fixed in 3% phosphate buffer glutaraldehyde at pH 7.4 and temperature 4°C for 24 hours and processed to get semithin sections stained with toluidine blue and examined by the light microscopy and ultra-thin sections[26] examined by TEM (JEM-1400 plus, Tokyo, Japan) respectively at the Faculty of Science, Alexandria University.

Statistical analysis

Data were fed to the computer and analysed using IBM SPSS software package version 20 (Armonk, NY: IBM Corp). For normally distributed quantitative variables and to compare more than two groups, ANOVA test was used. On the other hand, a Post Hoc test (Tukey) was performed for pairwise comparisons. The obtained results were considered significant at $p\ value \leq 0.05$[27].

RESULTS

Characterization of the isolated rat BM-MSCs

Morphological characterization of BM-MSCs by phase contrast inverted microscope

Two to three days after the initial seeding (p0), the cells were adherent and spindle in shape. At day 10 of p0, the spindle-shaped cells increased in number until they reached 80% confluency. Further passages at p1, p2 &p3 resulted eventually in cells with 85%, 90% & 95% confluency respectively with more homogenous fibroblast-like cells (Figures 1 A,B,C).

Colony forming unit-fibroblast (CFU-F) assay of BM-MSCs stained with crystal violet

Using the phase contrast inverted microscope, small stained colonies appeared on day 14 of p3. Each well that contained 100 cells gave about 92%± 1.04 colonies (Figure 1D).

Immunophenotyping of BM-MSCs by flow cytometer

Analysis of cell surface markers of BM-MSCs at p3, using monoclonal antibodies against MSC markers (CD44-PE and CD90-FITC) and another antibody against hemopoietic marker (CD45-PE), revealed that 92.02% of cells were positive for anti-CD44 and 96.11% of cells were positive for anti-CD90, while only 0.17% of cells were positive for anti-CD45 (Figures 1 E,F).

Biochemical results

MyoD and sTnI

An insignificant difference was detected in the mean levels of tissue MyoD in the control and the untreated injured groups ($p \geq 0.05$). On the other hand, the mean levels of tissue MyoD revealed significant increases in the PRP and the BM-MSCs-treated groups compared to the control and the untreated injured groups ($p \leq 0.05$). However, this elevation was significantly higher in the BM-MSCs-treated group than in the PRP group as $p \leq 0.05$ (Table 1, Figure 2A). On the other hand, there was a significant increase in the tissue level of sTnI in the untreated injured group compared to the other experimental groups ($p \leq 0.05$). Although treatment with PRP resulted in significantly lower level of sTnI than the untreated injured group, the reduction was still significantly higher than the control and BM-MSCs-treated groups ($p \leq 0.05$). In comparing the BM-MSCs-treated group and the control one, no significant difference was detected as $p \geq 0.05$ (Table 1, Figure 2B).

Oxidant and antioxidant markers

A significantly higher tissue MDA level was measured in the untreated injured group in comparison with all other experimental groups ($p \leq 0.05$). Even though treatment with PRP resulted in a significant reduction in the MDA level compared to the untreated injured group, the level was still significantly higher than the control and the BM-MSCs-treated groups. Meanwhile, a significantly higher level of MDA was detected in BM-MSCs-treated groups compared to the control one (Table 1, Figure 2C). On the other hand, a significantly lower levels of SOD, GSH and TAC were detected in the untreated injured group compared to all other experimental groups ($p \leq 0.05$). Although significantly higher levels of SOD, GSH and TAC were measured in the BM-MSCs-treated group than the PRP-treated group ($p \leq 0.05$), the levels in the BM-MSCs-treated group were still significantly lower than the control ($p \leq 0.05$) (Table 1, Figures 2 D-F).

Histological results

H&E stain

Group I (Control): Examination of longitudinal sections of the rat quadriceps femoris muscle of this group showed parallel cylindrical muscle fibers with acidophilic sarcoplasm and evident regular striations. Their nuclei were multiple, flattened, and peripherally situated beneath the sarcolemma (Figure 3).

Group II (Untreated injured group): Examination of the adult rats' quadriceps femoris muscles of this group revealed obvious structural changes. Most of the skeletal muscle fibers appeared disorganized. They exhibited disruption, discontinuity, and rupture. Others displayed a wavy pattern with dark peripheral nuclei. Some myofibers showed splitting and branching. Cellular infiltration was seen together with variable degrees of migrating pale-stained nuclei toward the site of injury. Centrally situated pale nuclei were encountered. Subsarcolemmal pyknotic nuclei were also detected. Extravasation of the red blood corpuscles as well as congested blood vessels with evident perivascular thickening and cellular infiltration was observed. A widened endomysium was noticed (Figures 4A-D).

Group III (PRP-treated): Examination of the rat quadriceps femoris muscle of this group revealed areas of apparently normal muscle fibers with peripheral flattened nuclei together with areas of interrupted myofibers and damaged sarcolemma. Split and branched fibers were observed. Some Myofibers were pale stained while others showed loss of the normal sarcoplasmic morphology. Some fibers displayed sarcoplasmic vacuolation. Rows of pale staining oval nuclei were seen traversing the muscle fibers towards the site of injury. Multiple nuclei were noticed accumulating in between as well as within the muscle fibers together with centrally situated nuclei. Widening of the endomysium was also encountered in some areas (Figures 5A-D).

Group IV (BM-MSCs-treated): The rat quadriceps femoris of this group showed mostly normal parallel cylinders of muscle fibers with acidophilic sarcoplasm and peripheral flattened nuclei. A narrow endomysium was also noticed. Split and branched muscle fibers were still encountered. Centrally situated nuclei were observed within some muscle fibers. On the other hand, some

myofibers depicted a mass of cellular proliferation together with rows of pale nuclei. Some fibers showed areas of pale sarcoplasm while a few fibers were still disrupted. (Figures 6A-D).

Masson's trichrome stain

Examination of Masson's trichrome-stained sections of the control rat quadriceps femoris muscles (group I) displayed a normal pattern of distribution of collagen fibers in the endomysium as well as in the perimysium. Meanwhile, the untreated injured group (group II) showed a deposition of an excessive amount of collagen fibers in between the injured myofibers. The PRP-treated group (group III) exhibited thick bundles of collagen fibers deposited in between the damaged skeletal muscle fibers and around the congested blood vessels. On the other hand, BM-MSCs treatment in group IV resulted in an almost normal pattern of collagen deposition where apparent minimal collagen fibers were depicted in the endomysium and the perimysium (Figures 7 A-D).

Morphometric analysis of Masson's trichrome-stained sections showed that the percentage area occupied by collagen was significantly higher in the untreated injured group than in the control group ($p \leq 0.05$). Treatment with PRP resulted in an insignificant reduction in the percentage area of collagen in comparison to the untreated injured group II ($p \geq 0.05$). Meanwhile, a significantly higher percentage area of collagen was detected in the PRP group compared to the control ($p \leq 0.05$). On the other hand, BM-MSCs injection in group IV led to a significant reduction in the percentage area covered by collagen compared to the PRP-treated as well as the untreated injured groups ($p \leq 0.05$), nevertheless, it was still significantly higher than that of the control group (Table 1, Figure 2G).

Semithin sections stained with toluidine blue stain

Examination of semithin sections of the control rat quadriceps femoris muscle (group I) showed parallel cylindrical muscle fibers, invested by a sarcolemma with sub-sarcolemmal flattened nuclei and evident pattern of cross striations consisting of alternating dark and light bands occurring in register to each other. Each muscle fiber is surrounded by a narrow endomysium containing blood capillaries. On the other hand, the untreated injured group (group II) exhibited distorted muscle fibers with ill-defined or even lost striations, disrupted sarcolemma, vacuolations, some abnormal nuclei or centrally located pale nuclei, in addition to the deposition of fibrous tissue in the wide endomysium. In the PRP-treated group, most of the skeletal muscle fibers of this group displayed quietly apparent alternating dark and light bands, even though the striations were faint in some areas while they were interrupted in others. Sarcoplasmic vacuolations were also encountered. In contrast, the BM-MSCs-treated group showed apparently normal muscle fibers with obvious striations apart from the existence of some vacuolations (Figures 8 A-G).

Electron microscopic results

Group I (Control): Examination of the ultra-thin sections of the control quadriceps femoris muscle by electron microscopy revealed parallel myofibrils consisting of myofilaments that showed transverse cross striations. These striations consisted of alternating dark (A) and light (I) bands that were almost perfectly in register with each other. The A band was bisected by a pale band (H band), which in turn was bisected by a dense line (M line). The I band was bisected by a dense line (Z line). Normal sarcomere was seen between two successive Z lines. The muscle fiber was invested by a sarcolemma with subsarcolemmal elongated nuclei. The sarcoplasm appeared at the nuclear poles as well as in between the myofibrils. It contained mitochondria, glycogen granules, and profiles of sarcoplasmic reticulum. The triads were encountered at the junction between the A and I bands. Each one consisted of a transverse tubule (T-tubule) surrounded bilaterally by two terminal cisternae of the sarcoplasmic reticulum (Figures 9 A-C).

Group II (Untreated injured group): Ultrastructure examination of specimens of the rats' quadriceps femoris muscles of this group showed areas of normally striated myofibrils alternating with areas of myofibrillar loss, fibril disintegration, and fibrinolysis. Some myofibrils were not in register with each other. The subsarcolemmal nuclei appeared irregular in shape while centrally situated and euchromatic nuclei were also encountered. Some mitochondria exhibited disintegrated matrix while others depicted variable shapes and sizes. The sarcoplasm showed dilated profiles of sarcoplasmic reticulum together with some triads that were distorted or displayed dilated terminal cisternae. The endomysium revealed excessive deposition of collagen fibers. Eosinophils with their characteristic shape and granules were encountered (Figures 10A-G).

Group III (PRP-treated): The quadriceps femoris muscles of adult albino rats in this group exhibited mostly regularly arranged myofibrils with normal transverse striated patterns alternating with areas of myofibrillar loss and interrupted myofibrils together with loss of the normal alignment of the Z lines. Some irregular nuclei were seen. Large mitochondria were encountered both subsarcolemmal and in the interfibrillar spaces. Deposition of collagen fibers was observed in the endomysium. Migratory cells were found in the vicinity of the fibers (Figures 11 A-D).

Group IV (BM-MSCs-treated): The skeletal muscle fibers of adult albino rats in this group displayed apparent normal structure compared to the control group with a normal pattern of striations except for some degenerative foci. Few myofibrils were interrupted with fibrillar loss while others depicted myofibrillar disarrangement and splitting. The nuclei appeared euchromatic, flat, and subsarcolemmal. Mitochondria were found at the nuclear pole as well as in between the myofibrils. Triads were seen at the A- I junction. (Figures 12 A-C)

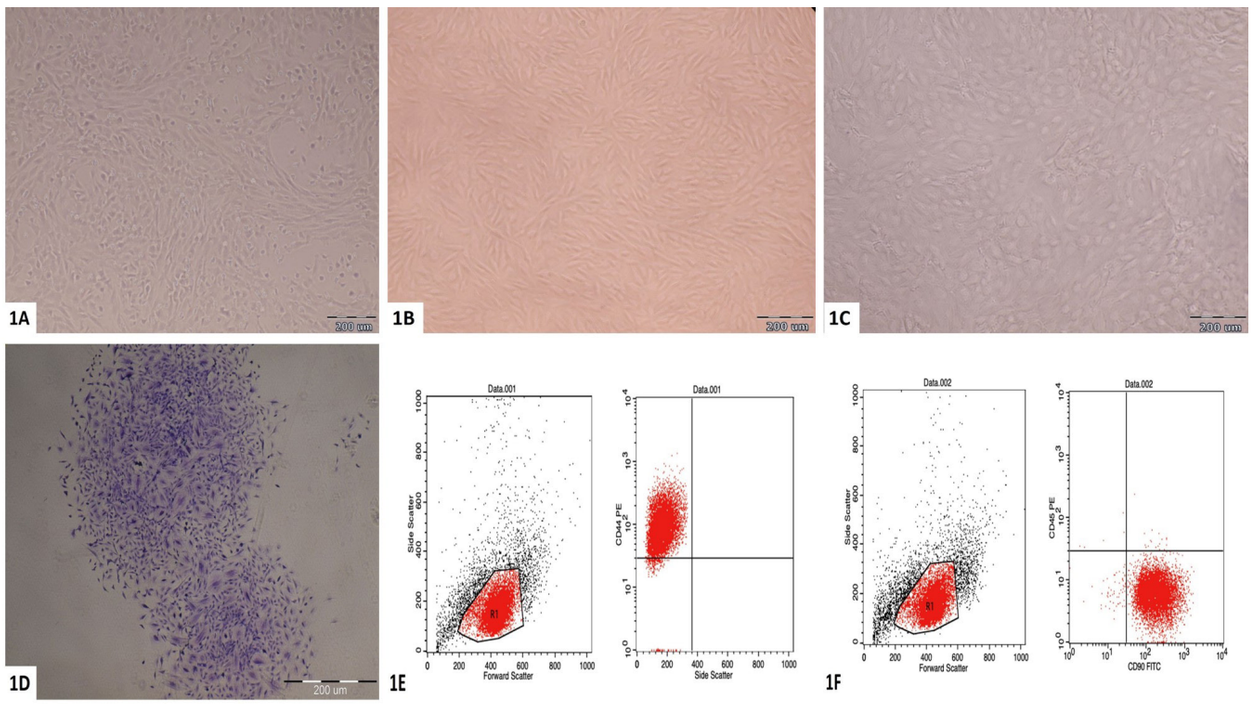

Fig. 1: A-F: A-D; Phase contrast inverted microscope of cultured BM-MSCs x100: A) Day 10 of p0 reveals 80% confluent cultured cells. B) p2 with 90% confluency. C) p3 with 95% confluency. D) CFU-F assay for p3 cultured cells with crystal violet stain, presenting colonies formation. E&F; A representative flow cytometric analysis of cell surface markers of BM-MSCs at p3: E) 92.02% of the cultured cells express the MSC marker (CD44) (upper left quadrant). F) 96.11% of the cultured cells express the MSC marker (CD90) (lower right quadrant), whereas only about 0.17% of the cultured cells are positive for the hemopoietic marker (CD45) (upper left quadrant).

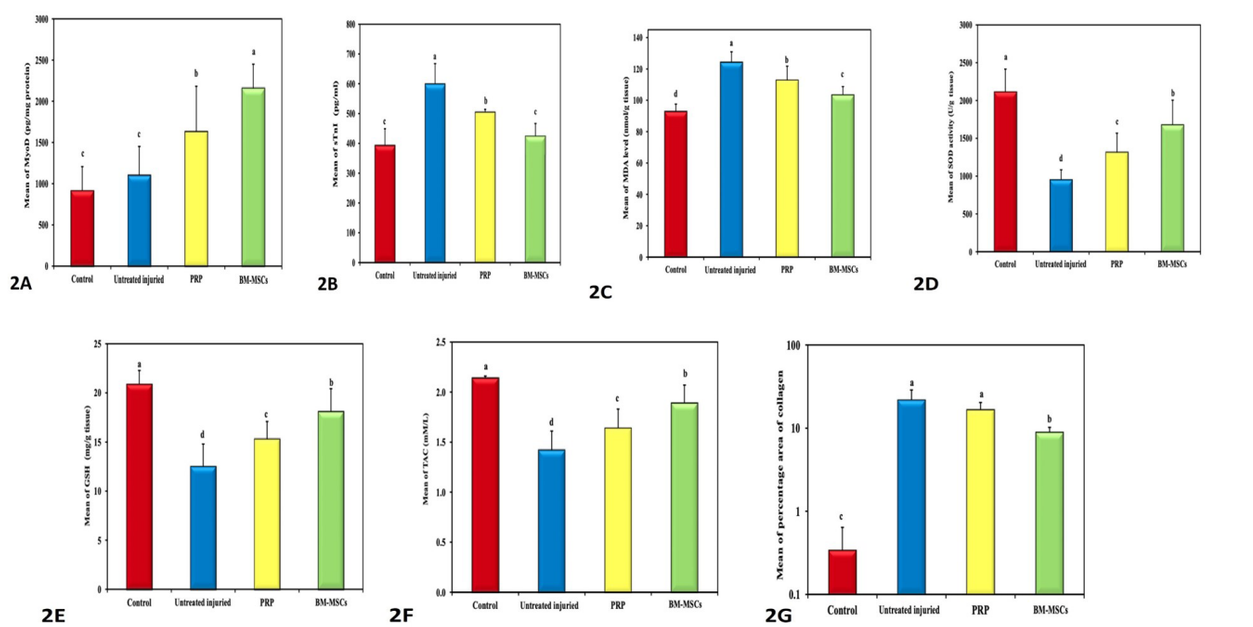

Fig. 2: A-G: Bar charts show A-F mean tissue levels of: A) MyoD in pg/mg protein, B) sTnI in pg/ml, C) MDA in nmol/gm tissue, D) SOD in U/g tissue, E) GSH in mg/g tissue & F) TAC in mM/L. G) Mean of percentage area of collagen.

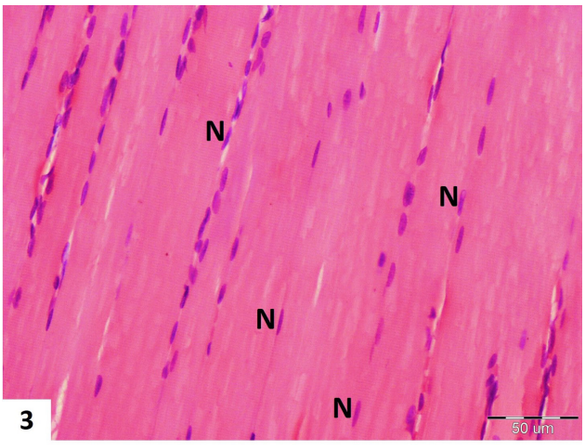

Fig. 3: A photomicrograph of a longitudinal section of a control rat quadriceps femoris muscle (group I) revealing parallel cylindrical muscle fibres with evident regular striations, acidophilic sarcoplasm, and multiple peripheral flattened nuclei (N). H&E X400

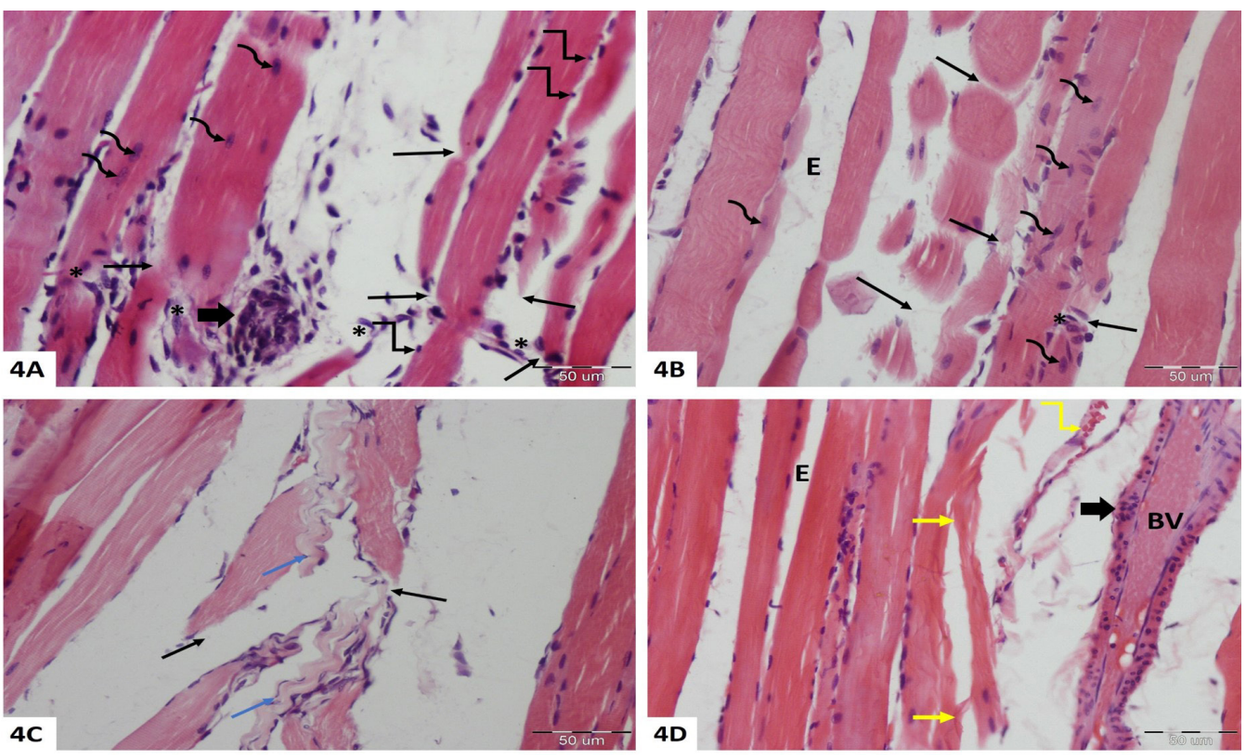

Fig. 4: A-D: Photomicrographs of longitudinal sections of a rat quadriceps femoris of the untreated injured group (group II). A) Disruption of the skeletal muscle fibres (arrows) with widened spaces between the muscle fibers occupied by dense cellular infiltration (thick arrow). Migratory cells with pale-stained nuclei (*) at the injured site, centrally situated pale nuclei (curved arrows) within the muscle fibers, and small dark nuclei (elbow arrows) beneath the sarcolemma, are all observed. B) Disruption and discontinuity of some muscle fibers (arrows), central pale-stained nuclei (curved arrows) within the muscle fibers together with migratory cells (*) toward the injured site. A widened endomysium (E) is noted. C) Discontinuity and rupture of the muscle fiber with ruptured sarcolemma (black arrows) together with disorganised wavy muscle bundles (blue arrows) that show faintly stained sarcoplasm with peripheral dark nuclei and complete loss of striations. D) Splitting and branching of the muscle fibres (yellow arrows), extravasation of red blood corpuscles (yellow elbow arrow) inside an injured muscle fiber, a congested blood vessel (BV) with perivascular thickening and infiltration (thick arrow). E; a widened endomysium. H&E X400

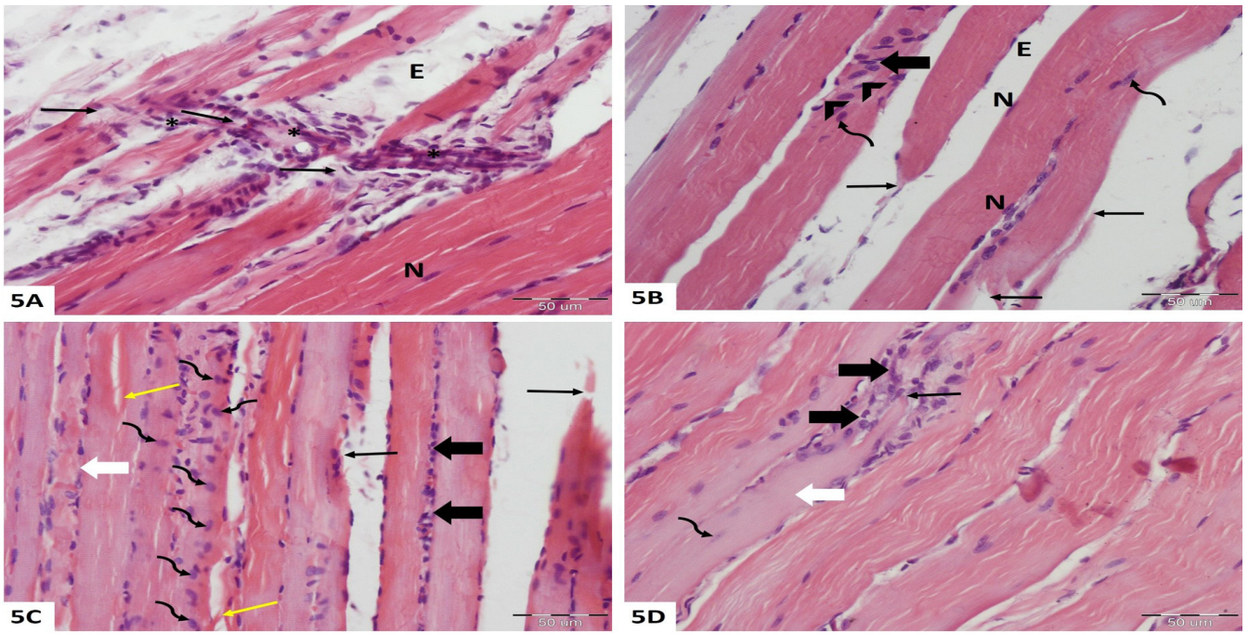

Fig. 5: A-D: Photomicrographs of longitudinal sections of rat quadriceps femoris muscles of the PRP-treated group (group III). A) Some apparently normal muscle fibers with peripheral flattened nuclei (N) while other muscle fibers are injured and interrupted (arrows) together with a large number of migrating cells toward the site of injury (*). E; a widened endomysium. B) Some apparently normal myofibers with subsarcolemmal flattened nuclei (N) together with discontinuity of other myofibers (arrows). Accumulation of cells with pale oval nuclei (thick arrow) and vacuolation (arrowheads) are noticed within some fibers. Curved arrows; centrally located pale nuclei. E; a widened endomysium. C) Areas of pale stained muscle fibers, some fibers are injured with damaged sarcolemma (black arrows) while others are split (yellow arrows) with loss of the normal sarcoplasmic morphology (thick white arrow). Rows of circular and flat nuclei (thick black arrows) in between the muscle fibers together with centrally situated pale nuclei (curved arrows) within the muscle fibers can be seen. D) Interruption of the muscle fibre (arrow) which shows pale homogenous sarcoplasm (thick white arrow) with a dense accumulation of cells within the site of injury (thick black arrows). Curved arrow; a centrally situated pale nucleus. H&E X400

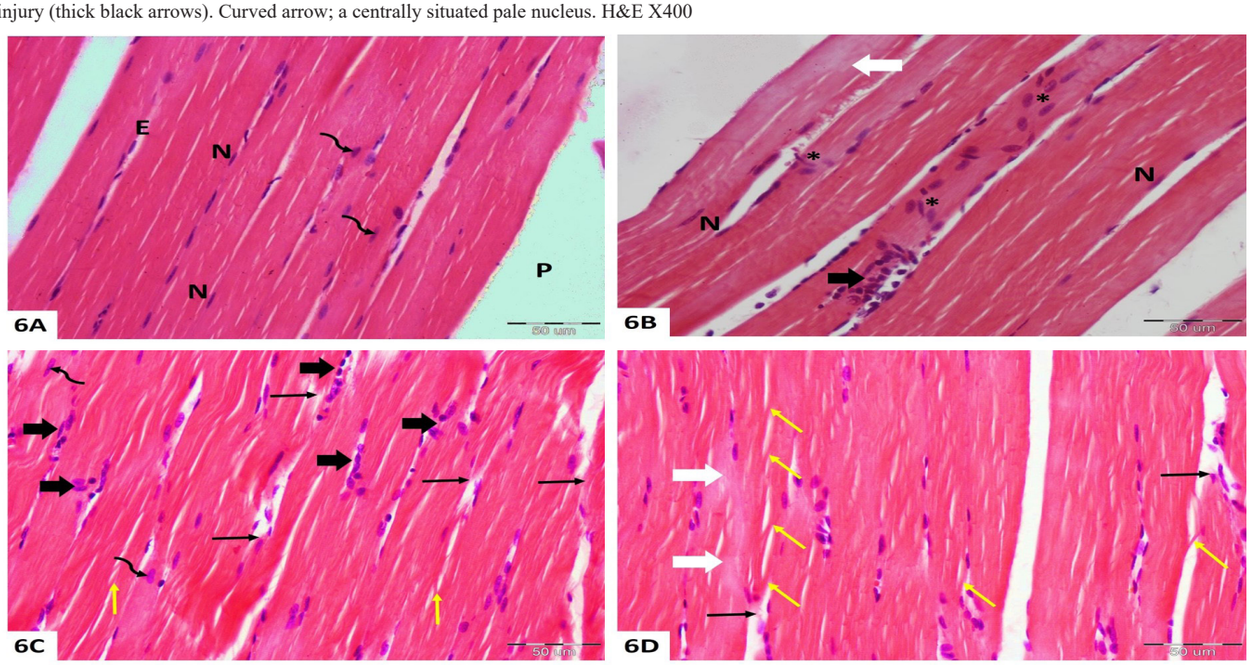

Fig. 6: A-D: Photomicrographs of rat quadriceps femoris muscles of the BM-MSCs-treated group (group IV). A) Area of normally appearing cylindrical muscle fibers with acidophilic sarcoplasm and peripheral flat nuclei (N). Each muscle fiber is surrounded by a narrow endomysium (E), while the bundles of muscle fibers are separated by the perimysium (P). Centrally situated pale nuclei (curved arrows) are encountered. B) Parallel cylinders of acidophilic muscle fibers with peripheral flattened nuclei (N). A mass of cellular proliferation (thick black arrow) and rows of pale staining nuclei (*) as well as areas of pale sarcoplasm with lost striations (thick white arrow) within some muscle fibers are noticed. C) Apparently normal muscle fibers with acidophilic sarcoplasm together with foci of disrupted muscle fibers (black arrows) as well as split and branched fibers (yellow arrows) can be seen. Accumulation of different types of cells (thick arrows) either in between or within the muscle fibers. Curved arrows; central pale nuclei within the muscle fibers. D) Parallel cylinders of apparently normal skeletal muscle fibers together with areas of disrupted myofibers (black arrows) are observed. Splitting and branching of the myofibers (yellow arrows) and areas with pale sarcoplasm (thick white arrows) are encountered. H&E X400

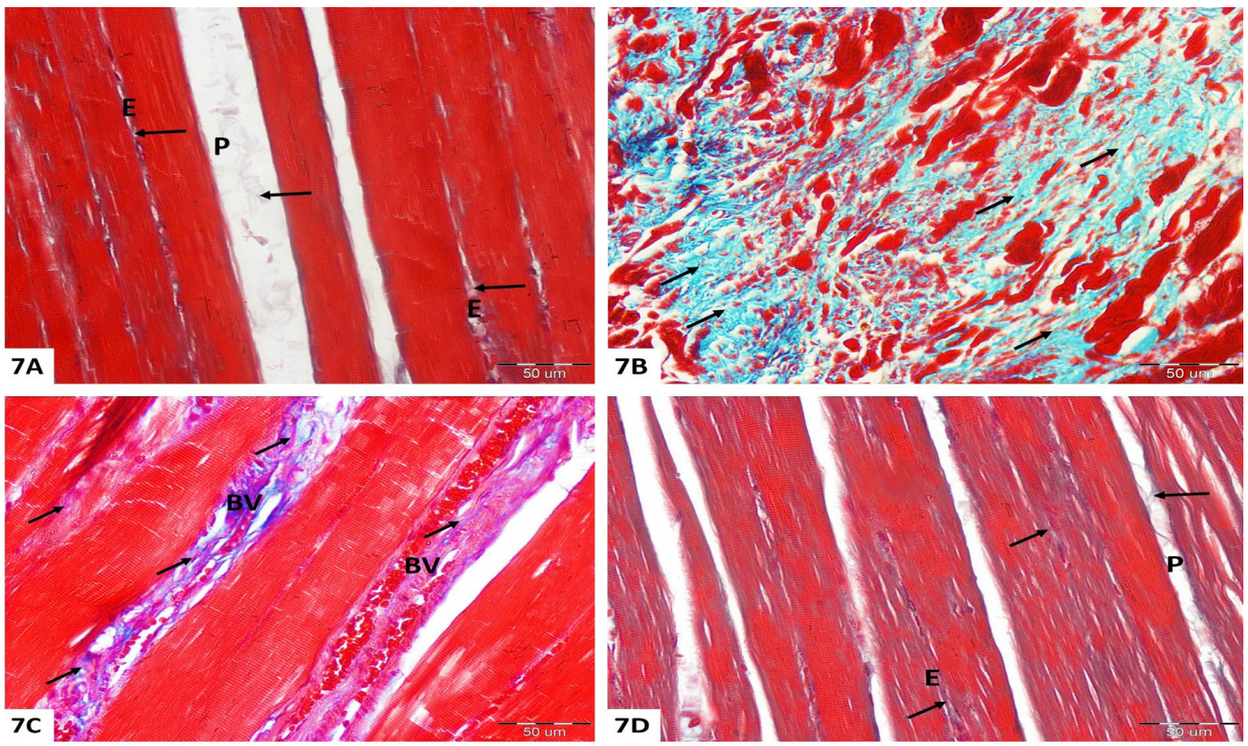

Fig. 7: A-D: Photomicrographs of longitudinal sections of rats' quadriceps femoris muscles. A) Control group (group I) shows parallel cylindrical muscle fibers with a minimum amount of collagen fibers (arrows) appear in the endomysium (E) and in the perimysium (P). B) Untreated injured group (group II) reveals excessive deposition of collagen fibers (arrows) in between the damaged muscle fibers. C) PRP-treated group (group III) exhibits deposition of thick bundles of collagen fibers (arrows) in between the injured muscle fibers and around the congested blood vessels (BV). D) BM-MSCs-treated group (group IV) shows a scanty amount of collagen fibers (arrows) deposited in the perimysium (P) as well as in the endomysium (E). Masson's trichrome X400

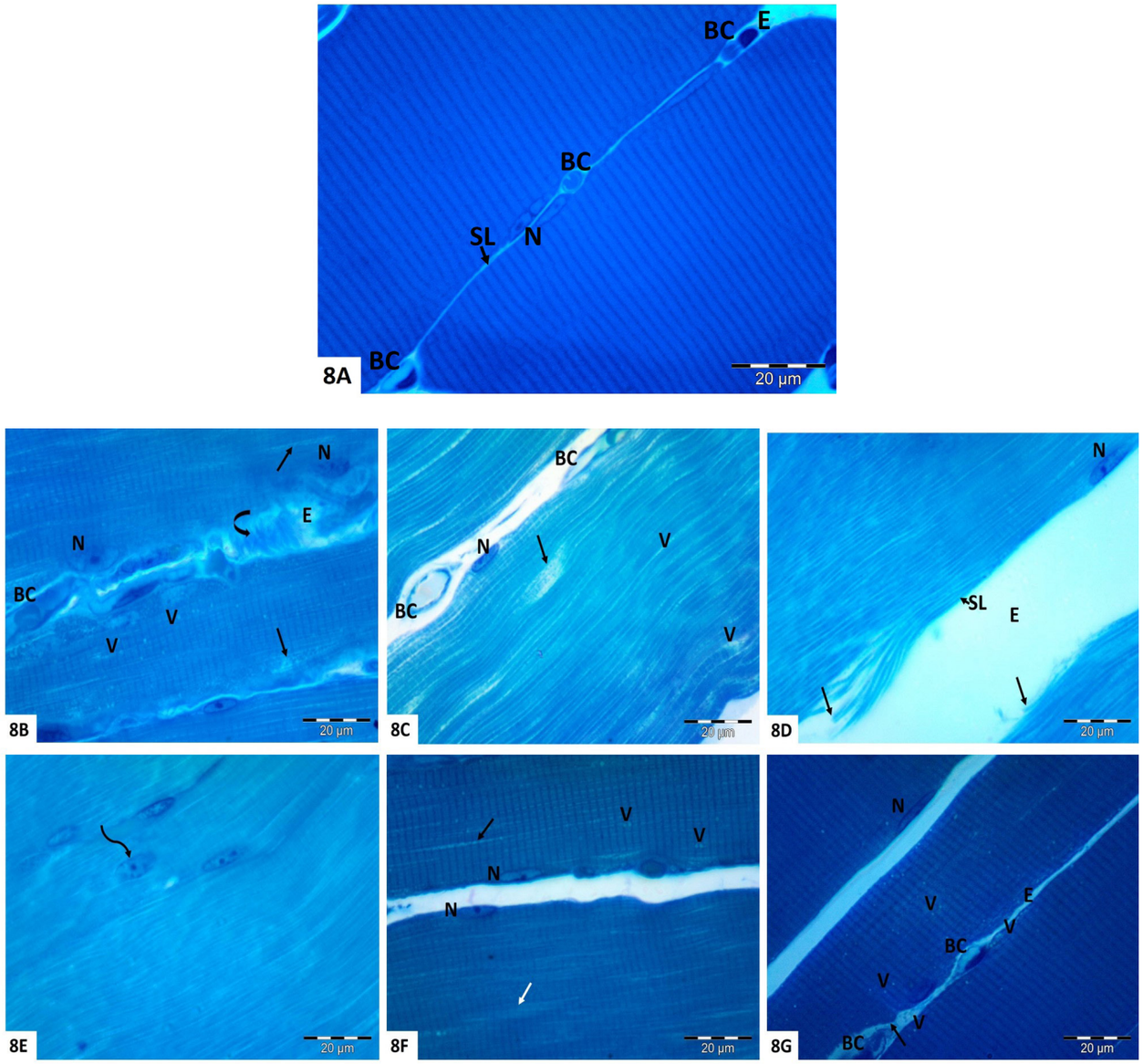

Fig. 8: A-G: Photomicrographs of semithin sections of the adult albino rats' quadriceps femoris muscles. A) Control group shows closely packed cylindrical muscle fibers with flattened and pale nuclei (N) situated underneath the sarcolemma (↑SL). The muscle fibers depict evident transverse striations consisting of alternating dark and light bands with multiple blood capillaries (BC) are seen in the endomysium (E). B-E; Untreated injured group: B) Distorted muscle fibers with areas of dissolution (arrows), irregularly shaped nuclei (N), and multiple vacuoles (V). The endomysium (E) reveals excess deposition of fibrous tissue (curved right arrow). BC, blood capillary. C) Muscle fibers with almost complete loss of striations with areas of dissolution (arrow) and vacuolations (V). N; subsarcolemmal nucleus, BC; blood capillaries. D) Disrupted muscle fibers (arrows), with complete loss of striations and injured sarcolemma (↑SL). E; a widened endomysium, N; nucleus. E) A centrally situated pale nucleus (curved arrow) within a muscle fiber that shows lost striations. F) PRP-treated group reveals striated muscle fibers with faint transverse striations in one area (white arrow) while they are interrupted in another one (black arrow) with sarcoplasmic vacuolations (V). N; nucleus. G) BM-MSCs-treated group shows cylinders of parallel muscle fibers with the normal pattern of striations and peripherally situated flattened nuclei (N). Irregularity of the sarcolemma in some areas (arrow) and vacuolations (V) can be seen in the sarcoplasm. E; endomysium contains blood capillaries (BC). Toluidine blue X1000

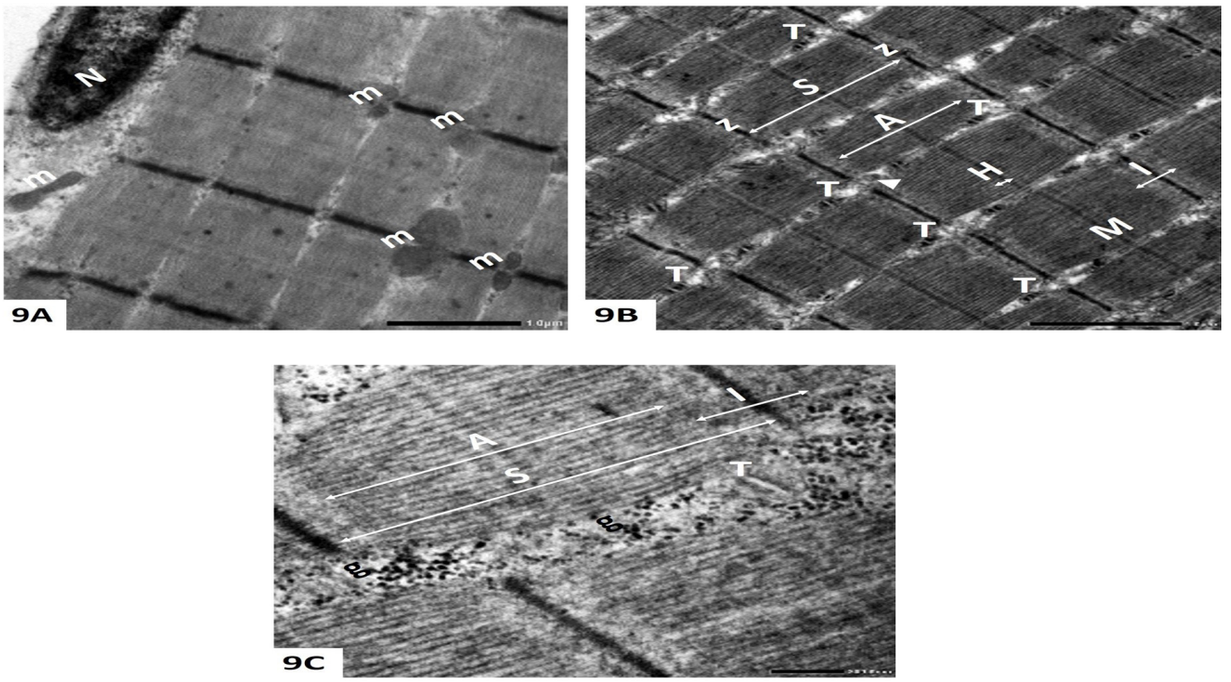

Fig. 9: A-C: Electron micrographs of a control rat (group I) quadriceps femoris muscles. A) Parallel myofibrils with alternating dark and light bands. A peripheral flat nucleus (N) is noticed under the sarcolemma and mitochondria (m) are depicted at the nuclear pole as well as in between the myofibrils. B) The myofibrils display alternating dark bands (A) and light bands (I). The A band is bisected by the H zone (H) which in turn is bisected by the M line (M). The I band is bisected by the Z line (Z). The sarcomere (S) occupies the distance between two successive Z lines. Evident triads (T) are noticed at the A-I junctions. Arrowhead; sarcoplasmic reticulum. C) A characteristic sarcomere (S) with multiple glycogen granules (g) are detected in between the myofibrils. T; a triad (T) at the A-I junction. A&B X 8000 & C X20.000

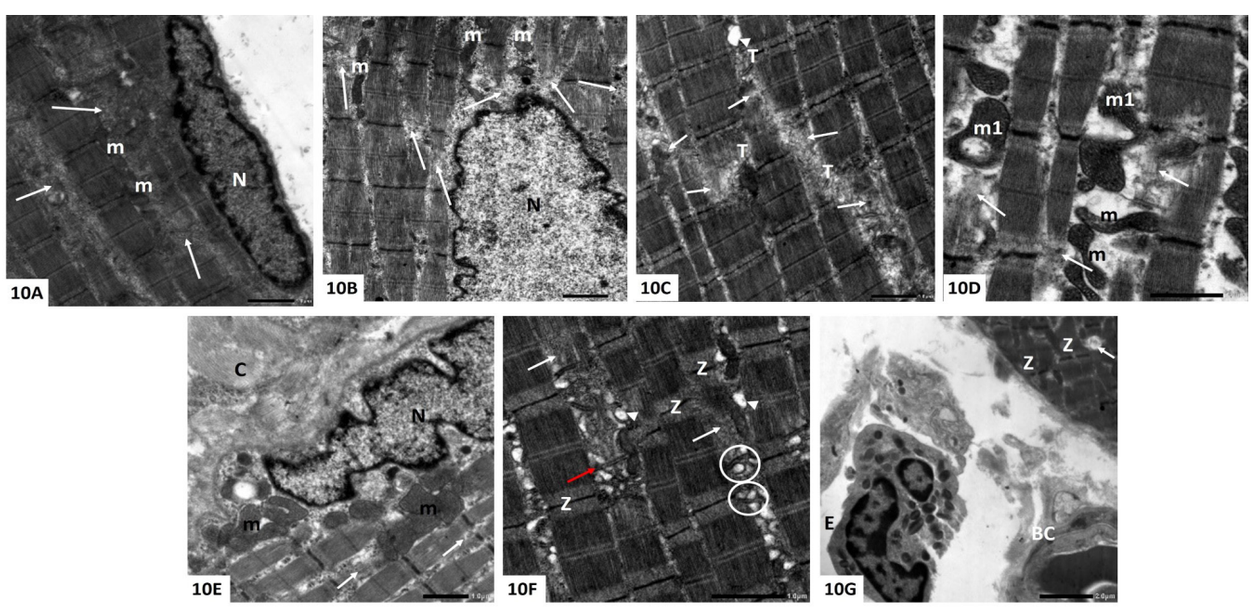

Fig. 10: A-G: Electron micrographs of rats' quadriceps femoris muscles of the untreated injured group (group II). A) A striated myofiber with focal areas of myofibrillar loss (arrows) occupied by mitochondria (m) with disintegrated matrix. An irregular nucleus (N) is seen under the sarcolemma. B) A part of a deeply situated euchromatic nucleus (N) surrounded with areas of myofibrillar lysis (arrows) that are occupied by mitochondria (m). C) Areas of myofibrillar disintegration (arrows) occupied by disorganized triads (T) with encountered dilated profiles of sarcoplasmic reticulum (arrowhead). D) Disorganized myofibrils with fibrillar disintegration (arrows). The mitochondria (m) acquire variable shapes and sizes, some show abnormal fusion (m1). E) A part of a myofiber with irregular nucleus (N) and focal lysis of the myofibrils (arrow). Pleomorphic mitochondria (m) are aggregated at the nuclear poles and in between the myofibrils together with excess deposition of collagen fibers (C) in the endomysium. F) Unregistered Z line (Z) with dilated profile of sarcoplasmic reticulum (arrowhead). The myofibrils are lost in some areas (white arrow) which are occupied by distorted triads (red arrow) while other triads exhibited dilated terminal cisternae (circle). G) A part of an injured myofiber with myofibrillar loss (arrow) and unregistered Z lines (Z). E; eosinophil with its characteristic nucleus and granules. BC; a blood capillary. A, B, C&E X5000, D&F X8000& G X3000

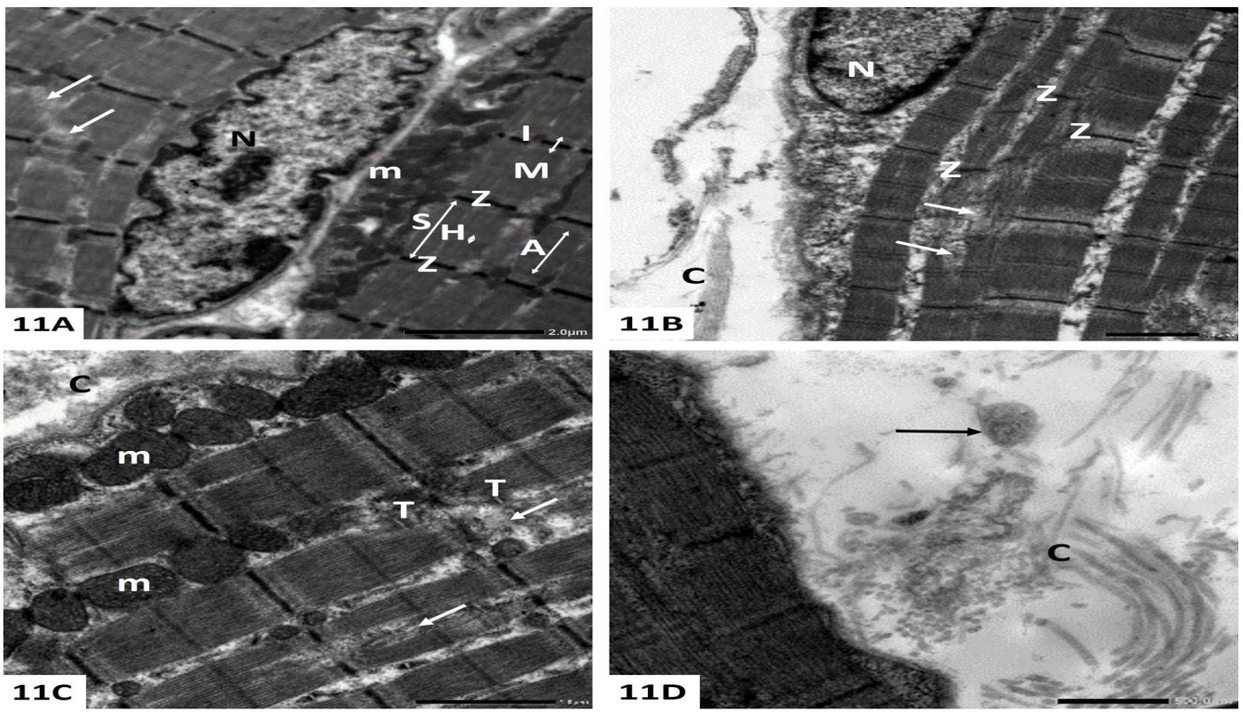

Fig. 11: A-D: Electron micrographs of rats' quadriceps femoris muscles of the PRP-treated group (group III). A) Areas of myofibrils with apparent normal transverse striation pattern, while others depict fibrillar loss (arrows) with subsarcolemmal irregular nucleus (N). m; multiple mitochondria beneath the sarcolemma. B) Interrupted myofibrils (arrows) with loss of the normal alignment of Z lines (Z). N; a part of a nucleus. C) Almost regularly arranged myofibrils with areas of myofibrillar loss and fibrinolysis (arrows). Large mitochondria (m) are noticed in the interfibrillar spaces as well as subsarcolemmal. T; triads. D) A migratory cell (arrow) in the vicinity of a part of a striated muscle fiber. C in B-D; collagen fibers in the endomysium. A&B X5000, CX8000& D X12.000

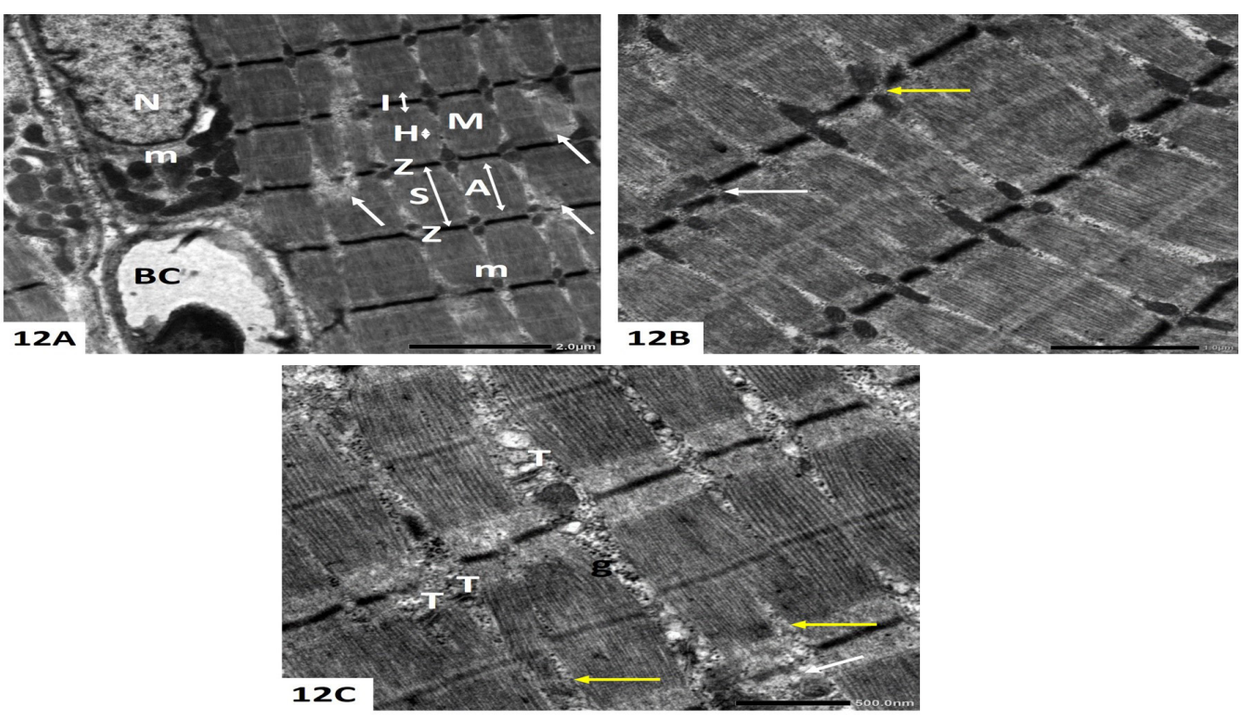

Fig. 12: A-C: Electron micrographs of rats' quadriceps femoris muscles of the BM-MSCs-treated group (group IV). A) Regularly arranged myofibrils with a normal pattern of cross striations and a part of an euchromatic flattened nucleus (N) is situated under the sarcolemma. Mitochondria (m) are seen at the nuclear poles and in between the myofibrils. Areas of interrupted myofibrils with myofibrillar loss (arrows) are depicted. BC; a blood capillary in the endomysium. S; sarcomere, A; dark band, I; light band, Z; Z line, H; H band & M; M line. B) Apparently normal myofibrils apart from a few foci of myofibrillar disarrangement (white arrow) and splitting (yellow arrow). C) Regularly arranged myofibrils with areas of myofibrillar splitting (yellow arrows) and disintegration (white arrow). Triads (T) are evident at A-I junctions. g; glycogen granules. AX5000, BX8000 & CX12.000

Table 1: Mean with Common letters are not significant (i.e. Means with Different letters are significant)

	Control	Injured-Untreated	PRP treated group	BM-MSCs treated group	F	*p*
MyoD (Pg/mg protein)						
Min. – Max.	504.0 – 1357.0	535.0 – 1453.0	890.0 – 2250.0	1573.0 – 2578.0	16.917*	<0.001*
Mean ± SD.	915.8^{c} ± 291.2	1102.9^{c} ± 348.0	1631.6^{b} ± 550.1	2158.5^{a} ± 291.1		
sTroponinI (Pg/ml)						
Min. – Max.	338.8 – 454.0	455.6 – 690.90	489.3 – 517.2	335.0 – 468.3	31.423*	<0.001*
Mean ± SD.	393.4^{c} ± 55.63	599.9^{a} ± 68.18	504.9^{b} ± 9.01	399.1^{c} ± 44.60		
MDA (mmol/g tissue)						
Min. – Max.	84.0 – 100.0	115.0 – 135.0	103.0 – 127.0	95.0 – 110.0	33.113*	<0.001*
Mean ± SD.	92.88^{d} ± 4.70	124.25^{a} ± 6.65	112.88^{b} ± 8.90	103.50^{c} ± 5.21		
SOD activity (U/g tissue)						
Min. – Max.	1563.0 – 2461.0	790.0 – 1188.0	1125.0 – 1900.0	1360.0 – 2170.0	28.712*	<0.001*
Mean ± SD.	2116.1^{a} ± 300.2	952.9^{d} ± 130.1	1315.1^{c} ± 253.2	1679.8^{b} ± 324.6		
GSH (mg/g tissue)						
Min. – Max.	18.40 – 22.50	9.80 – 16.90	12.80 – 18.50	14.80 – 20.80	26.337*	<0.001*
Mean ± SD.	20.89^{a} ± 1.39	12.51^{d} ± 2.29	15.30^{c} ± 1.79	18.10^{b} ± 2.33		
TAC (mM/L)						
Min. – Max.	2.10 – 2.17	1.22 – 1.66	1.40 – 1.96	1.69 – 2.22	29.712*	<0.001*
Mean ± SD.	2.14^{a} ± 0.02	1.42^{d} ± 0.19	1.64^{c} ± 0.19	1.89^{b} ± 0.18		
Area % covered by collagen						
Min. – Max.	0.07 – 0.67	14.23 – 31.83	11.66 – 19.80	5.99 – 10.44	44.723*	<0.001*
Mean ± SD.	0.34^{c} ± 0.30	21.87^{a} ± 6.93	16.65^{a} ± 3.65	8.94^{b} ± 1.27		

8 replica for each group SD: Standard deviation

F: F for One way ANOVA test, Pairwise comparison bet. each 2 groups was done using Post Hoc Test (Tukey)

p: p value for comparing between the different studied groups

*: Statistically significant at $p \leq 0.05$

DISCUSSION

In sports, muscle injuries are considered one of the most common injuries with over 90% of all these injuries are either contusions or strains[28]. The healing of a skeletal muscle injury tracks a properly consistent pattern, firstly; the inflammatory phase, secondly; the repair phase, and thirdly; the remodelling phase[29]. It is worth mentioning that the previous pattern of muscle regeneration is mainly reported in muscles subjected to low levels of strain. Nevertheless, severe injury, manifested by intense inflammatory response can disrupt this paradigm, resulting in excessive fibrosis formation with muscle dysfunction[30].

Regenerative medicine has recently emerged as a promising field in medical sciences that can repair tissue or organs damage caused by diseases or traumas[31]. So far, there are two competing technologies, specifically platelet-rich plasma (PRP) and stem cell therapies, which can restore the injured tissues[32]. In such a context, the present study aimed to compare the therapeutic effect of PRP versus BM-MSCs on the healing of an induced acute skeletal muscle injury in a rat model.

The chosen period of the whole experiment was three weeks, a period advocated by many previous studies for two reasons; firstly, it permits a sufficient time for the subsidence of the acute inflammatory phase and start of repair process,[33,34] and secondly, to allow recognition of any accelerated healing that would happen due to the used therapies[4].

In the current work, the light microscopic examination of the untreated injured group revealed obvious structural changes consistent with the muscle damage with limited signs of regeneration. In H&E stained sections, most of the skeletal myofibers appeared injured and interrupted with pyknotic nuclei. Other fibers appeared wavy with pale acidophilic sarcoplasm. Some displayed splitting and branching. Cellular infiltration, migratory cells with pale-stained nuclei together with deeply situated pale nuclei were encountered. Congested blood vessels and widened endomysium were depicted. Moreover, semithin sections revealed dissolution and vacuolation of the muscle fibers with lost striations and damaged sarcolemma.

The detected degenerative changes of the myofibers in this group were documented by various previous studies[35,36]. Ground *et al*[37] ascribed these changes to the direct mechanical force applied to the muscle that can lead to tearing the sarcolemma with subsequent sarcoplasmic affection resulting in the pale vacuolated appearance of the necrotic myofibers and the subsarcolemmal pyknotic nuclei. In addition, the sarcolemmal damage increases the sarcoplasmic calcium beyond the uptake capacity of the sarcoplasmic reticulum, ultimately destroying the excitation-coupling mechanism and causing activation of several proteolytic enzymes causing not only excessive muscle damage and lysis but also activation of various pathways of the complement system that results in formation of membrane attack complexes, eventually, inevitable membrane damage and cell death occur[38].

Subsequently, the damage-associated molecular pattern and the activated complement system elicit local macrophages and mast cells to release elevated levels of cytokines that act as inflammatory mediators recruiting other inflammatory cells[39]. In agreement with our study, perivascular and perimyseal cellular infiltration was detected in the untreated injured group. A similar finding was also reported by Sakuma *et al*[34] where a mixture of cellular infiltrate was encountered in injured rat muscles at weeks 2 and 3 respectively. On the other hand, the other unusual cellular infiltrate noticed in the untreated injured group, in the current work, was in the form of migrating cells with pale nuclei seen towards the site of fibers damage. These cells could represent reviving satellite cells that migrate under the influence of stromal-derived factor-1; a chemokine released by various nearby inflammatory cells to promote homing of the satellite cells at the site of injury[40].

Noteworthy, the encountered congested blood vessels in the untreated injured group could be attributed to ischemia caused by the injury that resulted in capillary dilatation, damage and release of multiple chemotactic factors that led to further vasodilation and damage culminating in necrosis of the muscle fibers[41]. Consequently, restoration of the blood flow to the muscle triggers the accumulation of fluid in the peri-fibrillary region causing the widening of the endomysium, which was noticed in the present study. This ischemia as well, is the leading cause of dispersed appearance, pale sarcoplasm, and contracture of the myofibers[36,37].

Meanwhile, the results shown by the light microscopic examination in the untreated injured group came in line with the electron microscopic one which revealed abnormal myofibrils in the form of fibrinolysis, myofibrillar loss, and disorganization. In addition, the sarcoplasm displayed pleomorphic mitochondria with disintegrated matrix. The appearance of pleomorphic mitochondria occurs in response to cellular stress, in which mitochondria undergo morphological transitions regulated by dynamic processes of membrane fusion and fission and these transitions directly modify the mitochondrial function, involving the release of reactive oxygen species (ROS) following acute muscle injury[42]. Moreover, the observed distorted and dilated triads in our results could be attributed to either mechanical stress exerted upon the muscle or to an increase in the calcium influx following damage of the sarcolemma[43].

In the current study, Masson's trichrome-stained sections revealed excessive deposition of collagen fibers in between the injured muscle fibers in the untreated injured group, which was further confirmed by the electron microscopic examination and the morphometric analysis. Multiple growth factors are implicated in the occurrence of fibrosis following muscle injury,[44] particularly transforming growth factor-beta one (TGF-β1) released from infiltrating cells[11], which has been nominated as the leader factor in the fibrotic process. TGF-β1 has a direct effect on myoblasts, triggering their transformation to myofibroblasts[45]. Even though myoblasts primarily act to repair damaged muscle fibers, they will also synthesize a substantial amount of collagen contributing to muscle fibrosis[46].

Generally, alteration in the biochemical environment of the damaged sarcolemma could be reflected upon the muscle integrity[38]. On the molecular level, it has been shown that damaged muscle cell sarcolemma could be an additional source of producing ROS. The uncontrolled production of ROS in turn leads to more attacks of the lipid-based cell membrane producing a cycle of more free radical productions[47]. Accordingly, oxidative stress generated following muscle injury was assessed in the present work by measuring the tissue levels of oxidative stress products and antioxidant parameters. The results revealed that the level of MDA was significantly raised accompanied with significant reduction in SOD, GSH and TAC levels in the untreated injured group compared to the other experimental groups.

It has been postulated that MyoD is the earliest marker of myogenic commitment[48]. In quiescent satellite cells, its expression occurs at tremendously low levels, however, in response to muscle injury, the damaged muscle fibers together with the recruited inflammatory cells send signals that activate dormant satellite cells causing their migration to the injury site, where they proliferate and up-regulate MyoD expression which in turn directs satellite cells towards proliferation and differentiation[49,50]. In the same context, the tissue level of MyoD in the current work, although elevated in the untreated injured group as a result of muscle damage, it was significantly lower than the PRP and the BM-MSCs-treated groups, with an insignificant difference with the control one. This could be explained by the low generation potential of severely damaged muscle myofibers or due to a natural down-regulation of MyoD which occurs due to subsiding the inflammation after 3 weeks[50]. Additionally, in the present study, sTnI was also measured as a biomarker for detecting musculoskeletal injuries[51]. The results showed a statistically significant elevation in sTnI level in the untreated injured group compared to the other three experimental groups. Our results aligned with the evidence in the literature that even minor muscle fibre injuries, that were not associated with an elevation in creatine kinase activity, were obviously supported by 10-fold increases in sTnI recommending that sTnI is a valuable marker for early detection of skeletal muscle damage[52].

Owing to the limited ability of skeletal muscle to regenerate in severe injuries[53], other convenient and applicable alternatives have emerged in an attempt to achieve the maximum healing response with minimum side effects. The choice of platelet-rich plasma (PRP) as a potential therapy stems from basic science evidence on the use of PRP in muscle diseases on account of its ability to increase leukocyte recruitment, growth factor release, angiogenesis, and satellite cells proliferation in muscle injury models[54].

Histological examination of the PRP-treated group in the present study showed a mixed pattern of muscle regeneration, damage, and fibrosis. The H&E-stained sections showed normal muscle fibers alternating with interrupted ones. Split and branched myofibers, pale-stained fibers, and fibers with vacuolations were still encountered. Cellular infiltration, migrating cells, and centrally situated nuclei within the myofibers were also observed. Moreover, semithin sections showed areas of apparently normal fibers, although, faint striations and fiber dissolution were depicted. Ultrastructure examination showed mostly regular myofibrils together with areas of persistent degenerative foci of myofibrillar loss and interruption. Some large mitochondria, irregular nuclei and collagen deposition were depicted.

Similar histologic findings with a mixed picture of regeneration and damage were also encountered by many researchers in studying the effect of PRP on rats with induced skeletal muscle injury. Rtail *et al*[16] found that 28 days following injury in the PRP-treated rats, areas of necrosis and massive fibrosis were still noticed alternating with regenerating fibers. They credited the existence of regenerating fibers to the capacity of PRP to induce angiogenesis, which is one of the cornerstones for the occurrence of muscle regeneration. They also reported heavy infiltration of the endomysium with various inflammatory cells. Furthermore, Kunze *et al* and Dimauro *et al*[54,55] documented a similar picture of regenerating muscle fibers with rows of pale stained nuclei. They related this regeneration of muscle fibers to PRP activation of the quiescent satellite cells as proved by an increase in the amount of multiple transcription factors like MyoD and PAX.

In fact, PRP contains various growth factors[8,56] which stimulate the mitogenesis of mesenchymal cells, chemotaxis, and angiogenesis in injured skeletal muscle, subsequently, enhancing the regenerative process in the muscle fibers[57]. On the other hand, PRP also contains significantly higher concentrations of TGF-β which can limit the efficacy of the other beneficial growth factors[56]. Thus, in the present work, although the percentage area covered by collagen was reduced in the PRP-treated group, the value was insignificant compared to the untreated injured one, and significantly higher in comparison to the control and the BM-MSCs-treated groups. In a published study by Tonogai *et al*[58] on muscle fibrosis following skeletal trauma in rat models, the PRP group revealed a higher percentage of fibrotic tissue when compared to the untreated group, nonetheless, the difference between these two groups was insignificant.

In the current study, biochemical analysis further confirmed the histological results in the PRP-treated group. It showed significant elevation in MyoD level compared to the control and the untreated injured groups but this elevation was still significantly lower than the BM-MSCs-treated group. It was documented that treatment with PRP induces myoblasts to proceed into the myogenic differentiation by activating MyoD owing to its content of the vascular endothelial growth factor (VEGF); an angiogenic-stimulating factor, which has been reported to increase myoblast proliferation, while influencing differentiation through MyoD up-regulation[59].

Alternatively, the present study showed a significantly lower sTnI in the PRP-treated group than the untreated injured one, yet, this level was still significantly higher than the control and the BM-MSCs-treated groups indicating incomplete recovery of tissue damage. Similarly, MDA level revealed a significantly lower level in the PRP-treated group than in the untreated injured group, though, this reduction was significantly higher than the other two groups. On the other hand, the tissue levels of SOD, GSH, and TAC in the PRP-treated group showed a significant elevation compared to the untreated injured groups, yet, this level was still significantly lower than the control and the BM-MSCs-treated groups. PRP was documented to lessen the oxidative damage through modulation of mitochondrial dysfunctions and activation of nuclear factor erythroid 2-related factor 2 (Nrf2) antioxidant response signaling pathway which can reduce ROS production and raise the level of resistance to oxidation[60].

Noteworthy, the local injection of PRP delivery can lead to complications related to the injection site other than the fibrotic effect[10]. Also the great variability during PRP preparation leads to a lack of standardized protocol with inconsistency among its preparation in different labs[61]. These concerns have pushed the need for another more efficient therapeutic tool.

Stem cells owing to their capacity for indefinite cell renewal and differentiation to different cell lines have made them an attractive field in therapy for replacement and regeneration of lost tissues. In particular, bone marrow-mesenchymal stem cells (BM-MSCs) own a vast potential for multi-directional differentiation including myogenic and angiogenic differentiation, both required for muscle regeneration[12].

Consistent with the previous finding, histological examination of the BM-MSCs-treated group in the current work showed appreciable muscle regeneration with apparent normal restoration of muscle architecture apart from the existence of few degenerative foci. The H&E-stained sections displayed noticeable regenerating muscle fibers. Few fibers exhibited pale sarcoplasm. Rows of pale migrating nuclei, centrally situated pale nuclei, and masses of cellular proliferation were also encountered. In addition, semithin sections revealed normal muscle fibers albeit some vacuolations and sarcolemmal irregularity were still observed. Ultrastructure examination showed an apparent normal structure of the myofibrils with the normal pattern of striations. However, a few interrupted myofibrils and myofibrillar loss were quietly noticed.

The observed regeneration in the skeletal muscle fibers in the BM-MSCs-treated group was consistence with multiple studies[15,17]. Notably, the splitting and

branching of the myofibers together with the centrally located nuclei that were observed in the present study, are considered diagnostic features of muscle regeneration and characterize the process of myogenesis. Short and long-term regenerated muscle fibers undergo splitting and branching either following necrosis of mature muscle fibers; as an outcome of incomplete lateral fusion of the newly formed myotubes within the same basal lamina or due to cleavage of mature uninjured muscle fibers. On the other hand, the centrally located nuclei indicate the formation of myotubes during the reparative process of the skeletal muscles. Interestingly, split and branched muscle fibers persist along with the centrally situated nuclei during the process of muscle regeneration[37].

It was established that BM-MSCs undergo their regenerative capacity in skeletal muscle either by stimulating differentiation of the satellite cells that then cause regeneration of the muscle fibers or directly by fusing to the muscle fibers or that both mechanisms co-exist[62] Accumulating evidence shows that BM-MSCs exert their effect on muscle regeneration mainly via paracrine effect. BM-MSCs can secrete different trophic factors into the damaged muscle microenvironment to enhance the endogenous repairing mechanism of satellite cells and promote their myogenic differentiation[12].

Moreover, the capability of transplanted stem cells to reduce excessive muscle fibrosis could be explained by their ability to decrease the tissue level of TGF-β1[13]. Hence, the present study revealed a significantly lower percentage area of collagen in the BM-MSC-treated group compared to the untreated injured and the PRP-treated groups, although, this percentage was still significantly higher than the control. In agreement with our result, Jiang *et al*[63] documented that MSCs effectively reduced skeletal muscle fibrosis after acute compartment muscle injury in rats with an increased number and diameter of regenerated muscle fibers.

In addition, the biochemical results in the current work showed overall improvement in regenerative markers and reduction in oxidative stress in the BM-MSC-treated group. MyoD levels were significantly elevated in this group in comparison to all other groups indicating the regenerative potential of BM-MSCs. In parallel, the sTnI level was not significantly elevated in this group compared to the control group, reflecting the waning of the muscle damage following injection of MSC.

Concurrently, MSCs have been reported to lessen oxidative stress by various mechanisms including scavenging free oxygen radicals, increasing antioxidant defences, moderating the inflammatory response, and enhancing cellular respiration or even donating their mitochondria to defend injured cells. Moreover, MSCs can up-regulate glutathione reductase leading to improving the GSH-to total glutathione ratio. Surprisingly, glutathione reductase was found to be secreted by MSCs themselves via exosomes[64]. This came in agreement with the current work in which the MDA level was significantly lower in the BM-MSCs-treated group compared to the untreated injured and the PRP-treated groups, meanwhile, this value was still significantly higher compared to the control. In tandem, the levels of antioxidant enzymes of this group (SOD, GSH, and TAC) were significantly higher in comparison to the untreated injured and the PRP-treated groups, yet, the level in the BM-MSCs group was still significantly lower than the control. These results reflect an attempt to normalize the oxidative stress level in the milieu of injured muscle by MSCs[65].

Taking all these results from the present study into consideration, local injection of BM-MSCs showed improved muscle regeneration with less fibrosis, reduced oxidative stresses, and improved antioxidant capacity compared to the untreated injured and the PRP-treated muscle groups. These results indicated that BM-MSCs could be a better choice for use in skeletal muscle regeneration following a contusion injury than PRP injection.

CONCLUSION

BM-MSCs posses a superb regenerative effect than PRP in treatment of acute skeletal muscle injuries.

CONFLICT OF INTERESTS

There are no conflicts of interest.

REFERENCES

1. Isern-Kebschull J, Mechó S, Pruna R, Kassarjian A, Valle X, Yanguas X, *et al*. Sports-related lower limb muscle injuries: pattern recognition approach and MRI review. Insights Imaging. 2020;11(1):108-124. doi:10.1186/s13244-020-00912-4
2. Green B, Pizzari T. Calf muscle strain injuries in sport: A systematic review of risk factors for injury. British Journal of Sports Medicine.2017;51(16):1189–1194. doi:10.1136/bjsports-2016-097177
3. Laumonier T, Menetrey J. Muscle injuries and strategies for improving their repair. Journal of Experimental Orthopaedics.2016;3(1):15-24. doi: 10.1186/s40634-016-0051-7
4. Hardy D, Besnard A, Latil M, Jouvion G, Briand D, Thépenier C, *et al*. Comparative Study of Injury Models for Studying Muscle Regeneration in Mice. PLoS One. 2016;11(1):1-24. doi:10.1371/journal.pone.0147198
5. Hotfiel T, Seil R, Bily W, Bloch W, Gokeler A, Krifter RM, *et al*. Nonoperative treatment of muscle injuries - recommendations from the GOTS expert meeting. J Exp Orthop. 2018;5(1):24-35. doi:10.1186/s40634-018-0139-3
6. Scully D, Naseem KM, Matsakas A. Platelet biology in regenerative medicine of skeletal muscle. Acta Physiologica. 2018;223(3):1-38. doi:10.1111/apha.13071

7. Merimi M, El-Majzoub R, Lagneaux L, Moussa Agha D, Bouhtit F, Meuleman N, *et al*. The Therapeutic Potential of Mesenchymal Stromal Cells for Regenerative Medicine: Current Knowledge and Future Understandings. Front Cell Dev Biol. 2021;9:1-18. doi:10.3389/fcell.2021.661532
8. Ling M, Quan L, Lai X, Lang L, Li F, Yang X, *et al*. VEGFB Promotes Myoblasts Proliferation and Differentiation through VEGFR1-PI3K/Akt Signaling Pathway. International Journal of Molecular Sciences. 2021; 22(24):1-14. doi: 10.3390/ijms222413352
9. Tonogai I. Influence of Platelet Rich Plasma on the Skeletal Muscle Fibrosis after Limb Lengthening in Mice. Foot & Ankle Orthopaedics. 2020;5(4):1. doi: 10.1177/2473011420S00468
10. Salamanna F, Veronesi F, Maglio M, Della Bella E, Sartori M, Fini M. New and emerging strategies in platelet-rich plasma application in musculoskeletal regenerative procedures: General overview on still open questions and outlook. BioMed Research International. 2015;2015:1-24. doi:10.1155/2015/846045
11. Ismaeel A, Kim JS, Kirk JS, Smith RS, Bohannon WT, Koutakis P. Role of transforming growth factor-β in skeletal muscle fibrosis: A review. International Journal of Molecular Sciences. 2019;20(10): 2446-2461. doi:10.3390/ijms20102446
12. Wang Y hao, Wang D ri, Guo Y chen, Liu J yuan, Pan J. The application of bone marrow mesenchymal stem cells and biomaterials in skeletal muscle regeneration. Regenerative Therapy. Regen Ther. 2020;15:285-294. doi: 10.1016/j.reth.2020
13. Qin L, Liu N, Bao CL, Yang D zhi, Ma G xing, Yi W hong ,*et al*. Mesenchymal stem cells in fibrotic diseases-the two sides of the same coin. Acta Pharmacol Sin. 2023;44(2):268-287. doi: 10.1038/s41401-022-00952-0
14. Ninagawa NT, Isobe E, Hirayama Y, Murakami R, Komatsu K, Nagai M, *et al*. Transplantated Mesenchymal Stem Cells Derived from Embryonic Stem Cells Promote Muscle Regeneration and Accelerate Functional Recovery of Injured Skeletal Muscle. Biores Open Access. 2013; 2(4): 295–306. doi:10.1089/biores.2013.0012
15. Boulos AN, El-Agawany AMA, Awwad AEM, Fouad GMM, El-Rahman AGAMA. The effect of bone marrow mesenchymal stem cells on experimentally-induced gastrocnemius muscle injury in female albino rats. Egyptian Journal of Histology 2021;44(1):218–235. doi: 10.21608/ejh.2020.24878.1257
16. Rtail R, Maksymova O, Illiashenko V, Gortynska O, Korenkov O, Moskalenko P, *et al*. Improvement of Skeletal Muscle Regeneration by Platelet-Rich Plasma in Rats with Experimental Chronic Hyperglycemia. Biomed Res Int. 2020;2020:1-9. doi: 10.1155/2020/6980607
17. Moussa MH, Hamam GG, Abd Elaziz AE, Rahoma MA, Abd El Samad AA, El-Waseef DAA, *et al*. Comparative Study on Bone Marrow-Versus Adipose-Derived Stem Cells on Regeneration and Re-Innervation of Skeletal Muscle Injury in Wistar Rats. Tissue Eng Regen Med. 2020;17(6):887-900. doi:10.1007/s13770-020-00288-y
18. Kirkwood J. AVMA Guidelines for the euthanasia of animals. Animal Welfare. 2013;22(3):412–412.
19. Dashore S, Chouhan K, Nanda S, Sharma A. Preparation of Platelet-Rich Plasma: National IADVL PRP Taskforce Recommendations. Indian Dermatology Online Journal. 2021;12(7):S12–S23. doi: 10.4103/idoj.idoj_269_21
20. Alhadlaq A, Mao JJ. Mesenchymal stem cells: Isolation and therapeutics. Stem Cells and Development. 2004;13(4):436–448. doi:10.1089/scd.2004.13.436
21. Akiyama K, You YO, Yamaza T, Chen C, Tang L, Jin Y, *et al*. Characterization of bone marrow derived mesenchymal stem cells in suspension. Stem Cell Research and Therapy. 2012;3(5):40-53. doi: 10.1186/scrt131
22. Martins AA, Paiva A, Morgado JM, Gomes A, Pais ML. Quantification and Immunophenotypic Characterization of Bone Marrow and Umbilical Cord Blood Mesenchymal Stem Cells by Multicolor Flow Cytometry. Transplantation Proceedings. 2009;41(3):943–946. doi:10.1016/j.transproceed.2009.01.059
23. Park JW, Thomas SM, Wylie LJ, Jones AM, Vanhatalo A, Schechter AN, *et al*. Preparation of Rat Skeletal Muscle Homogenates for Nitrate and Nitrite Measurements. Journal of Visualized Experiments 2021;2021(173), doi: 10.3791/62427. doi:10.3791/62427
24. Bancroft JD, Layton C. The hematoxylins and eosin. In: Suvarna SK, Layton C, Bancroft JD, editors. Bancroft's theory and practice of histological techniques. 8th ed. London: Elsevier; 2019: 126-38.
25. Van De Vlekkert D, Machado E, d'Azzo A. Analysis of Generalized Fibrosis in Mouse Tissue Sections with Masson's Trichrome Staining. Bio Protoc. 2020;10(10):1-16. doi:10.21769/BioProtoc.3629
26. Ann Ellis E. Staining Sectioned Biological Specimens for Transmission Electron Microscopy: Conventional and En Bloc Stains. In: Kuo J, editor. Electron Microscopy Methods and Protocols: Humana Press; 2014: 57-72. doi:10.1007/978-1-62703-776-1_4
27. Kirkpatrick LA Feeney BC. A Simple Guide to IBM SPSS Statistics for Version 20.0. Student ed. Belmont Calif: Wadsworth Cengage Learning; 2013.
28. Gimigliano F, Resmini G, Moretti A, Aulicino M, Gargiulo F, Gimigliano A, *et al*. Epidemiology of Musculoskeletal Injuries in Adult Athletes: A Scoping Review. Medicina 2021;57(10):1118-1126. doi:10.3390/medicina57101118

29. Baghdadi MB, Tajbakhsh S. Regulation and phylogeny of skeletal muscle regeneration. Developmental Biology. 2018;433(2):200–209. doi:10.1016/j.ydbio.2017.07.026
30. Gardner T, Kenter K, Li Y. Fibrosis following Acute Skeletal Muscle Injury: Mitigation and Reversal Potential in the Clinic. J Sports Med.2020;2020:1-7. doi: 10.1155/2020/7059057
31. Finnoff JT. Regenerative Rehabilitative Medicine for Joints and Muscles. Current Physical Medicine and Rehabilitation Reports 2020;8(1):8–16. doi:10.1007/s40141-019-00254-3
32. Ramaswamy Reddy S, Reddy R, Babu Nc, Ashok G. Stem-cell therapy and platelet-rich plasma in regenerative medicines: A review on pros and cons of the technologies. Journal of Oral and Maxillofacial Pathology. 2018;22(3):367-374. doi: 10.4103/jomfp.JOMFP_93_18
33. Järvinen TAH, Järvinen M, Kalimo H. Regeneration of injured skeletal muscle after the injury. Muscles, Ligaments and Tendons Journal. 2014;3(4):337-345.
34. Sakuma Y, Miyagi M, Inoue G, Ishikawa T, Kamoda H, Yamauchi K, *et al*. Muscle injury in rats induces upregulation of inflammatory cytokines in injured muscle and calcitonin gene-related peptide in dorsal root ganglia innervating the injured muscle. Muscle Nerve 2016;54(4):776-782. doi: 10.1002/mus.25092
35. Liu J, Liao Z, Wang J, Xiang H, Zhu X, Che X, *et al*. Research on skeletal muscle impact injury using a new rat model from a bioimpact machine. Front Bioeng Biotechnol. 2022;10:1-13. doi:10.3389/fbioe.2022.1055668
36. Jaćević V, Nepovimova E, Kuča K. Toxic Injury to Muscle Tissue of Rats Following Acute Oximes Exposure. Scientific Reports. 2019;9(1): 1457-1469. doi: 10.1038/s41598-018-37837-4
37. Grounds MD. The need to more precisely define aspects of skeletal muscle regeneration. International Journal of Biochemistry and Cell Biology. 2014;56:56-65. Grounds MD. The need to more precisely define aspects of skeletal muscle regeneration. International Journal of Biochemistry and Cell Biology. 2014;56:56-65. doi:10.1016/j.biocel.2014.09.010
38. Tidball JG. Mechanisms of muscle injury, repair, and regeneration. Comprehensive Physiology 2011;1(4):2029–2062. doi:10.1002/cphy.c100092
39. Tu H, Li YL. Inflammation balance in skeletal muscle damage and repair. Frontiers in Immunology. 2023;14:1-14. doi:10.3389/fimmu.2023.1133355
40. Kowalski K, Kołodziejczyk A, Sikorska M, Płaczkiewicz J, Cichosz P, Kowalewska M, *et al*. Stem cells migration during skeletal muscle regeneration - the role of Sdf-1/Cxcr4 and Sdf-1/Cxcr7 axis. Cell Adh Migr. 2017;11(4):384-398. doi:10.1080/19336918.2016.1227911
41. Jacobsen NL, Norton CE, Shaw RL, Cornelison DDW, Segal SS. Myofibre injury induces capillary disruption and regeneration of disorganized microvascular networks. Journal of Physiology 2022;600(1):41-60. doi:10.1113/JP282292
42. Qualls AE, Southern WM, Call JA. Mitochondria-cytokine crosstalk following skeletal muscle injury and disuse: A mini-review. American Journal of Physiology - Cell Physiology 2021;320(5):C681–C688. doi:10.1152/ajpcell.00462.2020
43. Takekura H, Fujinami N, Nishizawa T, Ogasawara H, Kasuga N. Eccentric exercise-induced morphological changes in the membrane systems involved in excitation-contraction coupling in rat skeletal muscle. Journal of Physiology. 2001;533(2):571–583. doi:10.1111/j.1469-7793.2001.0571a.x
44. Darby IA, Zakuan N, Billet F, Desmoulière A. The myofibroblast, a key cell in normal and pathological tissue repair. Cellular and Molecular Life Sciences. 2016;73(6):1145-1157. doi:10.1007/s00018-015-2110-0
45. Li Y, Foster W, Deasy BM, Chan Y, Prisk V, Tang Y, *et al*. Transforming Growth Factor-β1 Induces the Differentiation of Myogenic Cells into Fibrotic Cells in Injured Skeletal Muscle: A Key Event in Muscle Fibrogenesis. American Journal of Pathology 2004;164(3): 1007–1019. doi:10.1016/s0002-9440(10)63188-4
46. Li Y, Huard J. Differentiation of muscle-derived cells into myofibroblasts in injured skeletal muscle. American Journal of Pathology. 2002;161(3):895–907. doi: 10.1016/S0002-9440(10)64250-2
47. Powers SK, Deminice R, Ozdemir M, Yoshihara T, Bomkamp MP, Hyatt H. Exercise-induced oxidative stress: Friend or foe? Journal of Sport and Health Science. 2020;9(5):415–425. doi:10.1016/j.jshs.2020.04.001
48. Zammit PS. Function of the myogenic regulatory factors Myf5, MyoD, Myogenin and MRF4 in skeletal muscle, satellite cells and regenerative myogenesis. Seminars in Cell and Developmental Biology. 2017;72:19–32. doi:10.1016/j.semcdb.2017.11.011
49. Yamamoto M, Legendre NP, Biswas AA, Lawton A, Yamamoto S, Tajbakhsh S, *et al*. Loss of MyoD and Myf5 in Skeletal Muscle Stem Cells Results in Altered Myogenic Programming and Failed Regeneration. Stem Cell Reports. 2018;10(3):956-969. doi:10.1016/j.stemcr.2018.01.027
50. Tian ZL, Jiang SK, Zhang M, Wang M, Li JY, Zhao R, *et al*. Detection of satellite cells during skeletal muscle wound healing in rats: time-dependent expressions of Pax7 and MyoD in relation to wound age. Int J Legal Med. 2016;130(1):163-172. doi:10.1007/s00414-015-1251-x

51. Onuoha GN, Alpar EK, Dean B, Tidman J, Rama D, Laprade M, *et al*. Skeletal troponin-I release in orthopedic and soft tissue injuries. Journal of Orthopaedic Science. 2001;6(1):11–15. doi:10.1007/s007760170018

52. Sun D, Hamlin D, Butterfield A, Watson DE, Smith HW. Electrochemiluminescent immunoassay for rat skeletal troponin I (Tnni2) in serum. Journal of Pharmacological and Toxicological Methods. 2010;61(1):52–58. doi:10.1016/j.vascn.2009.09.002

53. Fleming JW, Capel AJ, Rimington RP, Wheeler P, Leonard AN, Bishop NC, *et al*. Bioengineered human skeletal muscle capable of functional regeneration. BMC Biol. 2020;18(1):145-161. doi:10.1186/s12915-020-00884-3

54. Kunze KN, Hannon CP, Fialkoff JD, Frank RM, Cole BJ. Platelet-rich plasma for muscle injuries: A systematic review of the basic science literature. World Journal of Orthopedics. 2019;10(7):278–291. doi:10.5312/wjo.v10.i7.278

55. Dimauro I, Grasso L, Fittipaldi S, Fantini C, Mercatelli N, Racca S, *et al*. Platelet-rich plasma and skeletal muscle healing: a molecular analysis of the early phases of the regeneration process in an experimental animal model. PLoS One. 2014;9(7):1-13. doi:10.1371/journal.pone.0102993

56. Mosca MJ, Rodeo SA. Platelet-rich plasma for muscle injuries: game over or time out? Current Reviews in Musculoskeletal Medicine. 2015;8(2):145–153. doi: 10.1007/s12178-015-9259-x

57. McClure MJ, Garg K, Simpson DG, Ryan JJ, Sell SA, Bowlin GL, *et al*. The influence of platelet-rich plasma on myogenic differentiation. J Tissue Eng Regen Med. 2016;10(4):E239-E249. doi: 10.1002/term.1755

58. Tonogai I, Hayashi F, Iwame T, Takasago T, Matsuura T, Sairyo K. Platelet-rich plasma does not reduce skeletal muscle fibrosis after distraction osteogenesis. Journal of Experimental Orthopaedics. 2018;5(1):26-34. doi: 10.1186/s40634-018-0143-7

59. Deasy BM, Feduska JM, Payne TR, Li Y, Ambrosio F, Huard J. Effect of VEGF on the regenerative capacity of muscle stem cells in dystrophic skeletal muscle. Molecular Therapy. 2009;17(10):1788-1798. doi: 10.1038/mt.2009.136

60. Martins RP, Hartmann DD, de Moraes JP, Soares FAA, Puntel GO. Platelet-rich plasma reduces the oxidative damage determined by a skeletal muscle contusion in rats. Platelets. 2016;27(8):784–790. doi: 10.1080/09537104.2016.1184752

61. Dohan Ehrenfest DM, Rasmusson L, Albrektsson T. Classification of platelet concentrates: from pure platelet-rich plasma (P-PRP) to leucocyte- and platelet-rich fibrin (L-PRF). Trends in Biotechnology. 2009;27(3):158-167. doi: 10.1016/j.tibtech.2008.11.009

62. Andrade BM, Baldanza MR, Ribeiro KC, Porto A, Peçanha R, Fortes FSA, *et al*. Bone marrow mesenchymal cells improve muscle function in a skeletal muscle re-injury model. PLoS ONE. 2015;10(6):1-14. doi: 10.1371/journal.pone.0127561

63. Jiang X, Yang J, Liu F, Tao J, Xu J, Zhang M. Embryonic stem cell-derived mesenchymal stem cells alleviate skeletal muscle injury induced by acute compartment syndrome. Stem Cell Research and Therapy. 2022;13(1):313-329. doi: 10.1186/s13287-022-03000-0

64. Stavely R, Nurgali K. The emerging antioxidant paradigm of mesenchymal stem cell therapy. Stem Cells Translational Medicine. 2020;9(9):985–1006. doi: 10.1002/sctm.19-0446

65. Park CM, Kim MJ, Kim SM, Park JH, Kim ZH, Choi YS. Umbilical cord mesenchymal stem cell-conditioned media prevent muscle atrophy by suppressing muscle atrophy-related proteins and ROS generation. In *Vitro* Cellular and Developmental Biology - Animal. 2016;52(1):68–76. doi: 10.1007/s11626-015-9948-1

الملخص العربى

دراسة لمقارنة التأثير العلاجي للبلازما الغنية بالصفائح الدموية مقابل الخلايا الجذعية الوسطية المشتقة من نخاع العظم على الإصابة الحادة للعضلات الهيكلية في ذكور الجرذان البيضاء البالغة

رنا سعد[١]، وحيد ستيفانوس[١]، أنيسة ميليس[١]، سمر صبحى[٢]، ايمان نبيل[١]

[١]قسم الانسجة وبيولوجيا الخلايا، [٢]مركز التميز فى ابحاث الطب التجددى وتطبيقاته، كلية الطب، جامعة الإسكندرية

المقدمة: إصابات العضلات الهيكلية شائعة جدًا لدى الرياضيين، ومع ذلك، لا يوجد علاج فعال متاح حتى الآن. تم استخدام البلازما الغنية بالصفائح الدموية والخلايا الجذعية الوسطية في علاج الاضطرابات العضلية الهيكلية المختلفة ومع ذلك، فما زال الجدل قائما بشأن التأثير الضار لحقن البلازما الغنية بالصفائح الدموية بعد إصابة العضلات.

الهدف: المقارنة بين التأثير العلاجي للبلازما الغنية بالصفائح الدموية مقابل الخلايا الجذعية الوسطية المشتقة من نخاع العظم في علاج الإصابة الحادة في العضلات الهيكلية لدى الجرذان.

المواد والطرق: تم استخدام ٥٢ جرذًا بالغًا في الدراسة بأكملها:٣٢ جرذًا كمجموعات تجريبية، و١٠ جرذان لإنتاج البلازما الغنية بالصفائح الدموية و١٠ جرذان لعزل الخلايا الجذعية الوسطية. تم تمييز الخلايا الجذعية الوسطية شكليا وبواسطة مقياس التدفق الخلوي. تم تقسيم ال ٣٢جرذ بالتساوى الي : المجموعة الأولى (الضابطة)، وخضعت المجموعات الثلاث الأخرى لإصابات مستحثة بالعضلة الفخذية رباعية الرؤوس و لم تتبع بأى معالجة في المجموعة الثانية (المصابة و الغير معالجة)، أو متبوعة بعد ساعتين بحقن عضلي واحد من محلول البلازما الغنية بالصفائح الدموية فى المجموعة الثالثة) معالجة بالبلازما الغنية بالصفائح الدموية) أو الخلايا الجذعية الوسطية المشتقة من نخاع العظم في المجموعة الرابعة (معالجة بالخلايا الجذعية الوسطية) كلا على حدا. بعد ٢١ يوما، تم التضحية بالفئران و الحصول على العضلات لإجراء الفحوصات البيوكيميائية والنسيجية. تم استخدام متجانسات الأنسجة لقياس مستويات بروتين تحديد الأرومة العضلية ، والتروبونين الهيكليI، والمالونديالدهيد، وديسموتاز الفائق الاكسده، والجلوتاثيون المختزل والقدرة الإجمالية لمضادات الأكسدة. تم تجهيزعينات العضلات وفحصها بالمجاهر الضوئية والإلكترونية. خضعت المقاطع الملونة بصبغه ماسون ثلاثية الألوان للتحليل المورفومتري و تم إجراء التحليلات الإحصائية.

النتائج: نتج عن إصابات العضلات المستحثة تلف الألياف العضلية، وتجوفات ،و احتشاد خلوي، وتلف بغشاء الليف العضلي، ونوى غير طبيعية، وميتوكوندريا متعددة الأشكال، وثالوثيات مشوهة، وزيادة ملحوظة في ترسب الكولاجين، والتروبونين الهيكليI والمالونديالدهيد مع انخفاض في إنزيمات بروتين تحديد الأرومة العضلية والإنزيمات المضادة للأكسدة. أظهرت المجموعة المعالجة بـالبلازما الغنية بالصفائح الدموية مزيجًا من تلف العضلات وتجددها. وفي الوقت نفسه، كشفت الخلايا الجذعية الوسطية عن تجدد نسيجي أفضل بصرف النظر عن عدد قليل من البؤر التنكسية.

الاستنتاج: أظهر حقن الخلايا الجذعية الوسطية المشتقة من نخاع العظم تجددا ممتازا للعضلات مع تليف أقل مقارنةً بـالبلازما الغنية بالصفائح الدموية.